Final Technical Report

Project details

Title: Application of protein profiles to identify common mechanism groups of pyrethrins and pyrethroids

Contract: T10020

Contractors: Alan R Boobis and Robert J Edwards

Staff: Oduaghanju O Okoturo (RA)

Dates: 14th August 2006 – 13th August 2009

Contents

Summary 3
Experimental procedures 6
Pyrethoids 6
Other chemicals 6
Cells 7
Cell culture 8
Addition of pyrethroids to cultured cells 8
Assessment of cell viability using the MTT Assay 8
Noradrenaline release 8
Glucose uptake 8
Preparation of cell homogenates for SELDI-TOF-MS and GeLC-MS/MS. 9
SELDI-TOF MS 9
GeLC-MS/MS 9
LC/MS Data Analysis 10
Functional analysis of proteins 10
Objective 01: Treatment of cells with test compounds 11
Test compounds 11
Observations and Results 14
Functional effects 14
Objective 02: SELDI-TOF mass spectrometry analysis 16
Effect of pyrethroids on SH-SY5Y cells 19
Univariate analysis 19
Unsupervised multivariate data analysis: PCA of pyrethroid-treated SH-SY5Y cells 19
Supervised Multivariate Analysis 22
(i) Classification based on two groups comprising treatment with vehicle-control and treatment with any pyrethroid. 22
(ii) Classification based on type I and type II pyrethroids 24
(iii) Development of a novel classification model. 26
Effect of pyrethroids on SK-N-SH cells 33
Univariate analysis 33
Unsupervised data analysis 33
Supervised Multivariate Analysis 34
(i) Classification based on two groups comprising treatment with vehicle-control and treatment with any pyrethroid 34
(ii) Classification based on the effect of type I and type II pyrethroids. 34
(iii) A novel classification model based on the results obtained using SHS5Y cells. 34
Effect of pyrethroids on HFF-1 cells 39
Univariate analysis 39
Unsupervised data analysis 39
Supervised Multivariate Analysis 39
(i) Classification based on two groups comprising treatment with vehicle-control and treatment with any pyrethroid. 39
(ii) Classification based on type I and type II pyrethroids 39
(iii) A novel classification model based on the results obtained using SH-SY5Y cells. 39
Objective 03: Identification of pathways affected using proteomics 45
LC/MS Data Analysis 45
Objective 04: Confirmation of functional role of identified proteins 48
General discussion 58
Conclusions 59
References 60

Summary

Pyrethrins are natural insecticides derived from the flowers of *Chrysanthemum cinerariaefolium*. They consist of six active constituents; pyrethrin I, pyrethrin II, cinerin I, cinerin II, jasmolin I and jasmolin II (LaForge and Markwood , 1938, Metcalf 1995, Fortin et al., 2008). Pyrethrins exhibit chemical instability; their rapid degradation upon exposure to air or sunlight has limited their application (Soderlund 1992, Elliott et al., 1978). To overcome this problem pyrethroids were developed. Pyrethroids are synthetic pesticides based on the structure of the original pyrethrins but with modifications that improved both their chemical stability and insecticidal properties whilst maintaining a relatively low mammalian toxicity. Such properties increased the marketability of these compounds and since the 1970s they have been used widely in agriculture. Today, pyrethroids represent a diverse group of over 1000 pesticides varying in their insecticidal and toxicological properties and about 10-15 are presently used in the majority of preparations for a wide array of indoor and outdoor applications (*e.g.* for medicinal, veterinary and agricultural purposes (ATSDR, 2003)). Pyrethroids are effective against a wide range of insect and mite pests and have been mixed with other pesticides for a broad spectrum of pest control. Pyrethroids have also been mixed with piperonyl butoxide, a synergist (Casida, 1970), which enhances the effect of the active ingredient by retarding its metabolic inactivation.

Pyrethrins and pyrethroids act by causing rapid paralysis of flying insects, the majority of their acute systemic effects have been associated with their action on the nervous system. In insects their mode of action is interference with transmission of nerve impulses. In mammals pyrethroids have been shown to interact with and alter the kinetics of sodium channels by prolonging the open state of voltage-dependent sodium channels in nerve cells when they are in the excited state. This causes repetitive firing or a block in the depolarisation of the neuron leading eventually to cell death (Narahashi, 2000, Soderlund et al., 2002, Vijverberg et al., 1990).

Pyrethroids have been classified as Type I or Type II based on chemical structure and biological effects caused by high-dose acute exposures to laboratory rats (Brekenridge et al., 2009, Gammon et al., 1981, Gray, 1985, Lawrence et al., 1982, Coats 1990, Verschoyle et al., 1980). Type I pyrethroids resemble pyrethrins, they lack an α-cyano group on the phenoxybenzyl moiety, and in treated rats typically cause aggressive sparring, increased sensitivity to external stimuli, tremor (T-syndrome), elevated body temperature, coma, and death. Type II pyrethroids include an α-cyano group on the phenoxybenzyl moiety and in rats typically cause pawing and burrowing behaviour, profuse salivation, increased startle response, abnormal hind limb movements, coarse whole body tremors leading to sinuous writhing (choreoathetosis), reduced body temperature and colonic seizures (sometimes observed prior to death). Rats exposed to Type II pyrethroids have been said to experience CS-syndrome (from choreoathetosis and salivation). Animals which have been exposed to levels of pyrethroids lower than those that cause T- or CS-syndrome exhibit less overt signs of neurotoxicity (Crofton et al., 1988, Joy et al., 1989). Two α-cyano-pyrethroids, fenpropathrin and cyphenothrin, have been shown to trigger responses intermediate to those of T- and CS-syndrome and have been therefore been classified as type I/II or TS pyrethroids (Miyamoto et al., 1995, Wright et al., 1988).

Pyrethrins and pyrethroids possess relatively low mammalian toxicity because they are quickly deactivated and eliminated by metabolic processes (Miyamoto, 1976) and have therefore been widely adopted as insecticides for both home and commercial use (Macan et al., 2006, Metcalf, 1995). They are thought to pose relatively little hazard to mammals (including humans) through natural routes of exposure (air, food) or at levels likely to be encountered in the environment or resulting from the normal use of pyrethrin- or pyrethroid-containing formulations. However, acute toxicity can occur at high levels of exposure when these chemicals are taken in overdose or misused. On rare occasions, T- or CS syndromes occur in humans exposed to very high levels, whereas occupational exposure to low levels of pyrethroids may induce irritative skin symptoms such as paresthesia, blistering and burning (Bradberry et al., 2005). These effects are usually short lived, peaking within 3–6 hours following dermal exposure and subsiding by 12–24 hours. There is no evidence to suggest that long-term, low-level exposure of adults to pyrethroids results in impairment of neurological function.

In order to predict the risks to human health (Amweg et al., 2005) of exposure to residues of pyrethrins and pyrethroids in food and water, it is important to understand the mechanism of toxicity of these compounds and whether they act in a similar manner, particularly when considering the possible effects of combined exposure. Although pyrethroids have been shown to interfere with the normal function of the sodium channel this may not necessarily be the only factor involved in the neurotoxicity of these compounds. There is increasing evidence that more than one molecular target may be involved (additional cellular targets for these compounds, including voltage-sensitive calcium channels, GABA receptors and voltage gated chloride channels, have been proposed (Shafer and Meyer, 2004, Crofton et al., 1987, Hildebrand et al., 2004, Lawrence and Casida, 1983, Soderlund, 2002). However, if there is a single target the cumulative effects on human health resulting from exposure to a mixture of pyrethroids that have a common mechanism of toxicity needs to be addressed (Wolansky et al., 2009). Also, at present there is very little information about why some pyrethroids cause T-syndrome and others cause CS-syndrome in rats and whether this has any relevance to toxicity in humans.

Therefore, in the work described here, surface-enhanced laser desorption/ionization time of flight mass spectrometry (SELDI-TOF MS) (Issaq et al., 2003) has been used to compare and examine protein profiles of neuronal cells exposed to pyrethroids and vehicle-controls. SELDI-TOF MS is unbiased and makes no prior assumption about the mechanism(s) of toxicity, nor that a single target is necessarily involved. It is rapid, reproducible, quantifiable and allows direct sample comparison over a range of proteins with masses of 2.5 kDa – 100 kDa.

The purpose of this study was to investigate common mechanism groups (CMGs)[1] of pyrethroid neurotoxicity by comparing the intensities of the protein ions in the SELDI-TOF MS protein profiles (Tang et al., 2004) of pyrethroid treated neuronal and fibroblast cells with vehicle-control treated cells and to determine if the pyrethroids could be separated into common mechanism groups based on changes in the SELDI TOF MS protein profiles. These changes were evaluated by univariate (Student's t-test) and multivariate statistical analyses (principal component and discriminant function analysis) and also volcano plots (Cui and Churchill, 2003). Receiver Operating Characteristic (ROC) curves (Metz, 1978) were used to assess the performance of these analyses to accurately classify and discriminate between putative common mechanism groups. Univariate analysis of the relative levels of individual protein ions indicated that the effects were small and no clearly consistent effects of the pyrethroids were evident. Similarly, principal component analysis did not reveal any obviously outlying samples or groups of samples for any of the cell lines. However, supervised multivariate analysis did show that it was possible to build models on the basis of a single CMG for all pyrethroids compared to the vehicle control for each of the cell lines. Further analysis to determine if models could be produced based on *a priori* grouping into type I and type II pyrethroids was not successful for any of the cell lines. However, it was possible to produce a model based on the effects of two groups comprising α-cypermethrin, β-cyfluthrin, resmethrin and tetramethrin (termed: group A) and λ-cyhalothrin, deltamethrin, fenvalerate, fenpropathrin and cis-permethrin (termed: group B) on SH-SY5Y cells. This grouping was not evident in the effects on SK-N-SH cells, which is consistent with the lack of a functional effect on these cells (i.e. noradenaline release and glucose uptake), nor, as expected, in HFF-1 cells.

Proteomics, using liquid chromatography-tandem MS, was used to identify the proteins affected by the pyrethroids, reveal how the proteome of the cell responds to pyrethroids, deduce pathways involved in pyrethroid toxicity and investigate whether the pyrethroids acted similarly on these pathways or whether they affected different pathways. It was anticipated that the information obtained from the SELDI -TOF MS and LCMS pathway analysis would prove useful for classifying the compounds into common mechanism groups. Identification of potential biomarkers of pyrethroid neurotoxicity may form the basis of a new way of assessing response and might be useful for the development of cumulative risk assessments. This analysis was performed on SH-SY5Y cells treated with resmethrin, tetramethrin (from group A), deltamethrin and λ-cyhalothrin (from group B), compared with vehicle control. Comparison

[1] A "common mechanism group" comprises a group of compounds that toxicologically act sufficiently similarly that they will exhibit dose addition when there is combined exposure to more than member of the group. For example, they may act on a common receptor, enzyme or ion channel to cause toxicity.

between the mean normalised abundances of expressed proteins in the five treatment groups indicated statistical differences in the levels of 306 proteins (ANOVA, $p<0.05$). *Post hoc* analysis was performed by comparing calculated protein abundances in each of the pyrethroid treatment groups with those in the vehicle-control group. By comparing the effects of the compounds on the up or down regulation of individual proteins it was possible to establish several patterns of response to summarise the data. Four main patterns were recognised which consistently grouped together the effects of resmethrin with tetramethrin (group A) and deltamethrin with λ-cyhalothrin (group B). It was observed that many of the proteins affected are involved in nucleoside and nucleic acid metabolism. These findings are a useful contribution to understanding how the proteome of cells responds to pyrethroids as such information is lacking in the literature.

In conclusion, treatment of SH-SY5Y cells with a variety of pyrethroids appeared to produce different effects on the protein profile which suggests they may comprise more than one CMG. Further work would be necessary to define the membership of such CMGs and to determine the mechanism(s) that cause the changes in protein expression and their biological consequences.

The specific objectives of the planned programme of work were:

Objective 01: Treatment of cells with test compounds

Objective 02: SELDI-TOF mass spectrometry analysis

Objective 03: Identification of pathways affected using proteomics

Objective 04: Confirmation of functional role of identified proteins

Experimental procedures

Pyrethoids*:* Allethrin (33396), α–cypermethrin (PS2083), β–cyfluthrin (PS1090), *cis*-permethrin (PS7581), deltamethrin (PS2071), fenvalerate (F1428), fenpropathrin (PS2002), λ-cyhalothrin (PS2018), resmethrin (PS1000) and tetramethrin (PS1042) were obtained from Sigma–Aldrich Company Ltd (Gillingham, UK). The structure of these compounds is shown in Figure 1.

Figure 1. Pyrethroid test compounds used in this study they have been classified as Type I or Type II based on differences in their chemical structure. Type I pyrethroids lack an α–cyano group on the phenoxybenzyl moiety, and type II pyrethroids include an α–cyano group on the phenoxybenzyl moiety.

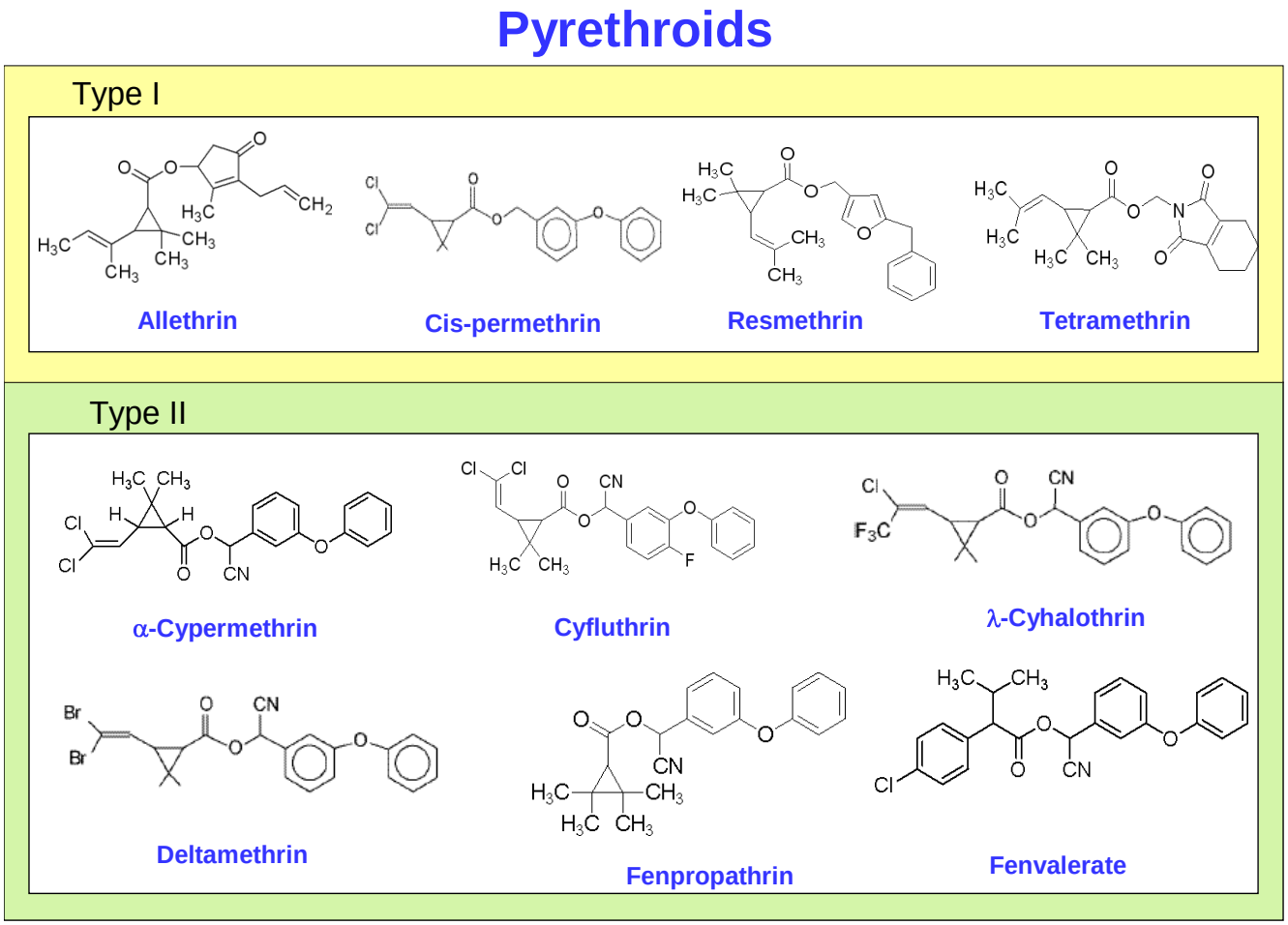

Other chemicals*:* DMEM (D5796), penicillin-streptomycin (P0781) trypsin-EDTA (T4049), trypan blue (T8154), HEPES buffer (H3375), D-glucose (G8270), KCl (P9333), PBS (P4417), desmethylimipramine (D3900), thiazolyl blue tetrazolium bromide (M5655), glycine electrophoresis reagent (G8898), perchloric acid, 70%, (311421), pargyline HCl (P8013), ammonium persulphate (A3678), ammonium bicarbonate (11213), Trizma hydrochloride (T3253), triton X-100 (234729), sodium chloride (57653), sinapic acid (85429) and N,N,N,N-tetramethylethylenediamine ~99% TEMED (T9281) were obtained from Sigma–Aldrich Company Ltd (Gillingham, UK). FBS (10106-169) and lithium dodecyl sulphate (LDS) buffer (NP0007) were obtained from Invitrogen. $CaCl_2.2H_2O$ (437053L),

$MgSO_4.7H_2O$ (10151) and acetronitrile (152516Q) were obtained from BDH (Lutterworth, UK). [7,8-^{3}H]Noradrenaline (TRA584-250UCI) and 3-methyl-d-[1-^{3}H]glucose (TRK372-1MCI) were obtained from GE Healthcare (Chalfont St Giles, UK). Gold Star multi-purpose liquid scintillation cocktail (GS1) was obtained from Meridian Biotechnologies Ltd (Epsom, UK). Solutions of 20% SDS (EC-874) and ProtoGel (30% w/v Acrylamide: 0.8% w/v bis acrylamide) (EC-890) was obtained from National Diagnostics UK (Hessle, UK). Trifluoroacetic acid (PT56045) and dimethylformamide were obtained from Rathburn Chemicals Ltd (Walkerburn, UK). InstantBlue Coomassie Stain (ISB1L) was from Expedeon Limited (Harston, UK). LC-MS grade water (W/0112/17) was obtained from Fisher Scientific Ltd (Loughborough, UK). BCA protein assay kit (Product # 23228) was obtained from Perbio Science UK Ltd (Cramlington, UK). CM10 Protein Chip Arrays (C57-30075) were obtained from Bio-Rad Laboratories Ltd (Hemel Hempsted, UK). Sequencing modified grade trypsin was obtained from Promega (Southampton, UK). Protein mixture digest (lP/N 161088), 10 cm PicoFrit columns packed with ProteoPep™ II C18 300Å (PFC7515-PP2-10-3PK) and Protecol Cap Trap Columns 300 Å (2222054) were obtained from Presearch Ltd (Basingstoke, UK).

Cells*:* The human neuronal cell lines SH-SY5Y (CRL-2266) and SK-N-SH (HTB-11) were obtained from the American Type Culture Collection (through LGC Standards, Teddington, UK) and the human fibroblast HFF-1 cell line was a kind gift from Dr Anne Bishop (Imperial College London, UK).

SH-SY5Y cells were cultured in T-175 flasks in Dulbecco's minimum essential medium (DMEM) containing 10 % fetal bovine serum (FBS) and 1% penicillin streptomycin and maintained at 37^{o}C in an atmosphere of 5% CO_2 and 95% air. The medium was changed every 3 days and the cells were spilt every 6 days (when they had reached ~80% confluency). They were counted using trypan blue (the viability was typically greater than 75%) and seeded to a density of 1 x10^5 cells/ml in the T-175 flask which contained a maximum of 30 ml of DMEM containing 10 % fetal bovine serum (FBS) and 1% penicillin streptomycin. The same culture conditions were used for the SK-N-SH and HFF-1 cells.

Figure 2. Human cell lines used for assessing the effects of pyrethroids. The cells lines are SH-SY5Y,SK-N-SH and HFF-1. P indicates the passage number, i.e. the number of times the cells were grown to 80% confluent and then divided for further culture (magnification x100).

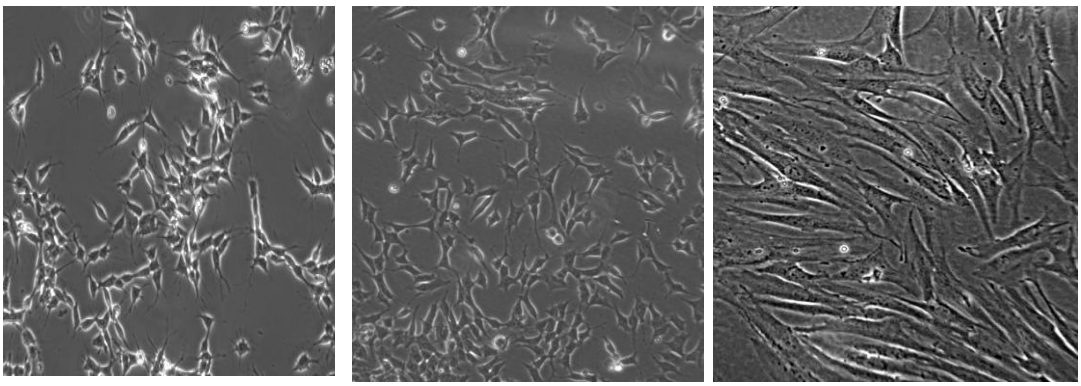

SH-SY5Y P-28 **SK-N-SH P-42** **HFF-1 P-5**

Cell culture*:* Cells were cultured in DMEM supplemented with 100 IU/ml penicillin, 100 μg/ml streptomycin and 10% foetal bovine serum (full growth medium) in a humidified atmosphere of 95% air and 5% CO_2 at 37°C. In some experiments cells were cultured without fetal bovine serum but with the other additions present (serum-free medium) (Figure 2).

Addition of pyrethroids to cultured cells*:* Test compounds were initially dissolved in DMSO and a series of stock concentrations of 1000-times strength prepared in DMSO. The stock solutions were then diluted 1000-fold into serum-free medium to the desired concentration, typically in the range of 0.5-100 μM pyrethroid (and 0.1% DMSO), that was added to cultured cells. DMSO stocks were kept stored at room temperature and diluted into medium freshly on each occasion

Assessment of cell viability using the MTT Assay*:* Cells were seeded into 96-well plates at a density of 5×10^5 cells/ml (SH-SY5Y cells) or 2×10^5 cells/ml (SK-N-SH and HFF-1 cells) in 100 μl of full growth medium and cultured for 3 days. The medium was then removed and replaced with 100 μl serum-free medium and returned to the incubator for 24 hours. The medium was removed from the cultured cells and replaced with 100 μl of the pyrethroid-containing medium or vehicle-control and incubated for a further 24 hours. Cell viability was determined by adding 25 μl of the tetrazolium salt substrate solution (5 mg/ml: 3-(4, 5-dimethylthiazol-2-yl)-2, 5-diphenyltetrazolium bromide (MTT) diluted in phosphate buffered saline) to each well for 1 h at 37°C. This was followed by 100 μl lysis buffer (10% SDS in 50% dimethylformamide) and incubation overnight. The absorbance of the purple cleavage formazan product was measured at 570 nm and quantified colorimetrically using a microtitre plate reader (Labsystems MultiScan RC, VWR International, UK). The MTT viability procedure was based on that described by Mosmann (1983). Cell viability was also assessed by trypan blue exclusion method for the SH-SY5Y cell line.

Noradrenaline release: All experiments were performed in triplicate. Cells were suspended at a density of 5×10^5 cells/ml (SH-SY5Y cells) or 2×10^5 cells/ml (SK-N-SH and HFF-1 cells) in serum-free medium and volumes of 1 ml transferred to sterile 15 ml polypropylene screw capped centrifuge tubes. Each of the pyrethroids was added in serum-free medium to a final concentration in the range of 10 – 100 μM (maximum tolerated concentration), as appropriate, in 0.1% (v/v) DMSO and then incubated for 24 hours. The medium was removed from cells following centrifugation at 1700 x g for 5 min at 4°C and replaced with 1 ml of uptake buffer (10 mM HEPES, 135 mM NaCl, 5 mM KCl, 0.6 mM $MgSO_4$, 2.5 mM $CaCl_2$, 0.2 mM ascorbic acid, 0.2 mM pargyline, 6 mM D-glucose, pH 7.4) containing 50 nM of [^{3}H]-labelled noradrenaline and incubated for 1 hour to allow uptake of noradrenaline. Excess noradrenaline was then removed from the cells by washing the cells by centrifugation as described above 5-times with 1 ml volumes of the uptake buffer containing 2nM desmethylimiprimine. The cells were then incubated in 1 ml of basal buffer (10 mM HEPES, 135 mM NaCl, 5 mM KCl, 0.6 mM $MgSO_4$, 2.5 mM $CaCl_2$, 0.2 mM ascorbic acid, 0.2 mM pargyline, 6 mM D-glucose, pH 7.4) for 5 minutes to allow release of noradrenaline and following centrifugation the supernatant was collected and transferred into a pre-labelled scintillation vial containing liquid scintillation cocktail (4 ml). Then, cells were suspended in 1 ml of potassium stimulated uptake buffer (basal buffer containing 135 mM KCl and 5 mM of NaCl in place of 5 mM KCl and 135 mM NaCl) and incubated for 5 min to allow further release of noradrenaline. Again, the supernatant was collected and prepared for scintillation spectroscopy. Finally, the cells were lysed with 2 M perchloric acid (1 ml) and also prepared for scintillation spectroscopy.

Glucose uptake: All experiments were performed in triplicate. Cells were prepared as described for the noradrenaline release experiments except that they were washed in 1 ml of uptake buffer (4 mM NaCl, 5.6 mM KCl, 2.3 mM $CaCl_2$, 1.0 mM $MgCl_2$, 3.6 mM $NaHCO_3$, 5 mM HEPES, 6 mM pyruvate and 4 mM D-glucose, pH 7.4) before incubation in the same buffer containing 1.1 μCi 3-O-methyl-d-[1-^{3}H] glucose (^{3}H-3-OMG) for 1 min. Following centrifugation the supernatant was removed and the pellet was rapidly washed with 1 ml of ice cold PBS (Mannerström and Tahti, 2004). The cells were lysed with 0.4 M NaOH (1 ml) overnight and then 200 μl 2 M HCl was added and the solution transferred to a pre-labelled scintillation vial containing Gold Star multi-purpose liquid scintillation cocktail (4 ml) and cpm determined over a period of 1 minute using a Wallac 1409 liquid scintillation counter.

Preparation of cell homogenates for SELDI-TOF-MS and GeLC-MS/MS: Cells were seeded into a series of 6-well plates at a density of 5×10^5 cells/ml (SH-SY5Y cells) or 2×10^5 cells/ml (SK-N-SH and HFF-1 cells) in 2 ml of full growth medium and cultured for 3 days during which time the cells adhered to the bottom of the wells achieving a confluency of ~70%. The medium was then removed and replaced with 2 ml serum-free medium and incubated for 24 hours. The medium was removed from the cultured cells and replaced with 2 ml of the pyrethroid-containing medium or vehicle-control-containing medium and incubated for a further 24 hours. The medium was then aspirated and the cells washed with 2 ml PBS before solubilisation in 100 µl 9M urea/2% CHAPS. Each sample was transferred to a 1.5 ml capped Eppendorf centrifuge tube for storage (at -80^{o}C). The protein content was determined using the bicinchoninic acid method (Perbio Science UK Ltd., Cramlington, UK).

Cell homogenates were diluted with 9M urea/2% CHAPS/5mM dithiothreitol to a protein concentration of 0.1 µg/µl for SELDI-TOF MS and 2 µg/µl for GeLC-MS/MS.

SELDI-TOF MS*:* Proteins in cell homogenates were analysed by Surface-Enhanced Laser Desorption/Ionization Time Of Flight Mass Spectrometry (SELDI-TOF MS) using weak cation exchange (CM10) ProteinChip arrays (BioRad, Hemel Hempstead, UK). The CM10 ProteinChips comprise 8 application spots allowing for 8 samples to be run in one array (Figure 3).

Figure 3 (a) Weak cation exchange (CM10) protein chip array it contains 8 active surfaces

Up to 12 Proteinchips were placed in a bioprocessor in a 96-well plate format and each was pre-treated with 200 µl binding buffer (0.1 M sodium acetate, pH 4) and incubated at room temperature for 5 min with shaking at 1050 rpm. The binding buffer was removed and the pre-treatment step repeated before addition of 90 µl binding buffer to each well. Cell homogenates were diluted to a protein concentration of 0.1 µg/µl in 9 M urea/2% CHAPS/5 mM dithiothreitol, allowed to stand at room temperature for 15 mintes and volumes of 10µl added to the wells of the bioprocessor. Each sample was analysed in duplicate. The samples were allowed to bind to the interactive surface of the ProteinChips for 1 h with shaking at 1050 rpm, after which unbound proteins and other material in the binding buffer were discarded and the wells washed for 5 min with fresh binding buffer (200 µl) twice with shaking at 1050rpm, followed by two washes with water (200 µl). The bioprocessor was then removed from the ProteinChips and the surfaces allowed to dry for 1 hour at room temperature. Then, 0.5 µl of a saturated solution of sinapic acid (an energy-absorbing molecule that aids ionisation of the proteins) in 50% acetonitrile and 0.5% trifluoroacetic acid was applied to each surface, and after allowing to dry for 30 min, a second application applied. The ProteinChips were then read on a Protein Biology System IIc Reader (Ciphergen Biosystems Inc., Freemont, CA, USA) using the following settings: laser intensity 250, detector sensitivity 10 and optimal molecular mass range 5000-30000 Daltons. Spectra were analysed using Biomarker Wizard software (Ciphergen). All ion peaks from m/z 5000 to 30000 with a signal to noise ratio above 2.5 were auto-detected and aligned within 0.3% of mass error. Data comprising mass (m/z) and ion intensity of each peak were exported to Excel spreadsheets where mean relative peak intensities were calculated and compared between pyrethroid treated and vehicle-control groups.

GeLC-MS/MS: The cell homogenates (50 µg) were prepared for 1D-SDS PAGE in lithium dodecyl sulphate buffer and reduced with 5 mM dithiothreitol with heating at 100°C for 2 min. The samples were then allowed to cool to room temperature and then alkylated with 250 mM iodoacetamide for 20 min in the dark at room temperature. The samples (45 µg) were then separated by SDS-PAGE using a 10% polyacrylamide gel and stained with Instant Blue overnight. Each of the gel lanes was sliced into 20 regions based on MW markers and the distribution of proteins in the samples. The gel pieces were de-colourised by placing each slice into a well of a 24-well plate (containing 0.5mL of 200 mM ammonium bicarbonate in 50% acetonitrile) with shaking at 600 rpm. The solution was removed after 1 hour and

replaced with fresh solution. The procedure was repeated until the gel pieces had de-colourised. The gel pieces were then washed with water (1 ml) for 5 minutes, and then dehydrated in acetonitrile (0.5ml) twice for 30 min with shaking at 600 rpm. The gel pieces were removed and placed into pre-labelled low binding Eppendorf 1.5 ml tubes and allowed to dry for 30 min. Proteins contained within each gel slice were digested in 0.3 ml of 50 mM ammonium bicarbonate containing 1 ng/µL trypsin at 37°C overnight. On the following day, tryptic peptides were extracted by addition of 0.3 ml 0.1% formic acid in 2% acetonitrile and mixed at 1050 rpm at 4^{o}C for at least 30 min. Then, 425 µl was removed and dried under vacuum for 12 hours at 38^{o}C. The dried peptide extract was dissolved in water containing 0.1% trifluoroacetic acid (30 µl) and transferred to an Agilent LC sample vial for LC-MS analysis using an Agilent 1200 series Nanoflow LC system linked to an LTQ linear ion trap MS (Thermo, UK). Samples of 2 µl were applied onto a Protecol Cap Trap Column at a flow rate of 10 µl/min and then separated by nano-LC using 10 cm PicoFrit column at a flow rate of 300 nl/min over a linear gradient of 0-54% acetonitrile containing 0.1% formic acid for 40 min. MS analyses of eluted peptides were recorded using a LTQ linear ion trap MS (Thermo, UK) connected to the nano-LC effluent through an electrospray interface.

LC/MS Data Analysis: MS data files were imported into Progenesis software (for LC MS version 2.5, Non-Linear Dynamics, Newcastle upon Tyne , UK) for comparative analysis of spectra and hence peptide and protein levels. Protein identification was performed using Bioworks Browser software, version 3.2 (Thermo-Fisher Scientific) and used SEQUEST to search for matches within the *Homo sapiens* Refseq protein database (National Center for Biotechnology Information 2008) and was based on identification of two or more peptides for each protein. Normalised abundance values were determined for each protein using Progenesis and differences between the vehicle-control and pyrethroid treated cells homogenates calculated (Student's t-test).

Functional analysis of proteins: Proteins of interest identified using Progenesis were entered into the PANTHER (Protein ANalysis THrough Evolutionary Relationships (http://www.pantherdb.org/)) Classification System and the proteins were categorised by molecular function and biological process.

Objective 01: Treatment of cells with test compounds

Each pyrethroid will be tested for its toxic effect on the cell lines to establish a workable range of concentrations that will be used for protein profile studies. Functional studies at the biochemical level on the cell lines will also be performed.

Test compounds*:* The compounds selected for study are illustrated in Figure 1 (allethrin, α-cypermethrin, β-cyfluthrin, cis-permethrin, deltamethrin, fenpropathrin, fenvalerate, λ-cyhalothrin, resmethrin and tetramethrin). They represent members of the different classes of compounds that have and are currently being used extensively for home, industrial and agricultural use.

Initial experiments were performed using the MTT reduction assay as an indirect measurement of cell number/viability to determine appropriate growth conditions. The basis of the MTT assay is the ability of mitochondrial dehydrogenase enzymes from viable cells to cleave the yellow tetrazolium MTT salt and form an insoluble dark blue formazan product, which can be solubilised and quantified colorimetrically. The number of surviving cells is proportional to the level of the formazan product created and the absorbance of the formazan product at 570 nm can be measured using a multi-well scanning spectrophotometer. A seeding concentration of $5x10^4$ SH-SY5Y cells/well was selected as suitable (Figure 4). The quantity of cells resulting after culture for 3 days was easily measurable and not overcrowded giving adequate latitude to determine increased or decreased growth rates following treatment with pyrethroids.

Figure 4. Relationship between MTT absorbance and number of cells seeded. Between $5x10^3$ and $5x10^6$ SH-SY5Y cells were seeded into 96-well plate wells and cultured for 3 days. MTT (25 µl/well of 5 mg/ml stock) was added to the cells which were returned to a 37^{o}C incubator for 1 hour before addition of 10%SDS/50% DMF for a further 2 hours. The absorbance of the formazan product at 570nm was measured using a microtitre plate reader.

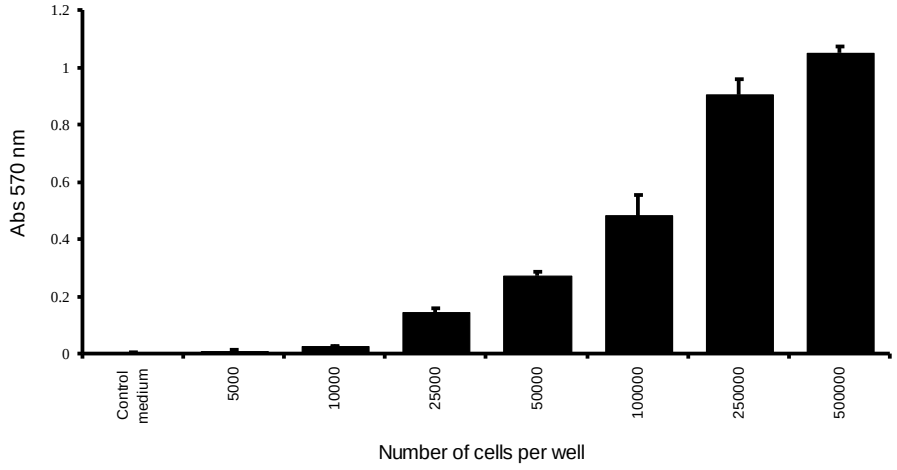

Figure 5. **Dose-dependent cytotoxicity of 10 pyrethroids on SH-SY5Y cells.** 5x10^4 cells/well were grown in 96 well plates for 3 days in serum containing medium. The medium was then replaced with serum-free medium and the cells were cultured for a further 24h, before addition of fresh serum-free medium containing one of each of 10 pyrethroids over a concentration range of 0.5-100 μM. After a further 24h, MTT reagents were added and the absorbance at 570 nm was recorded. * $P < 0.05$, ** $P < 0.01$, Student's t-test.

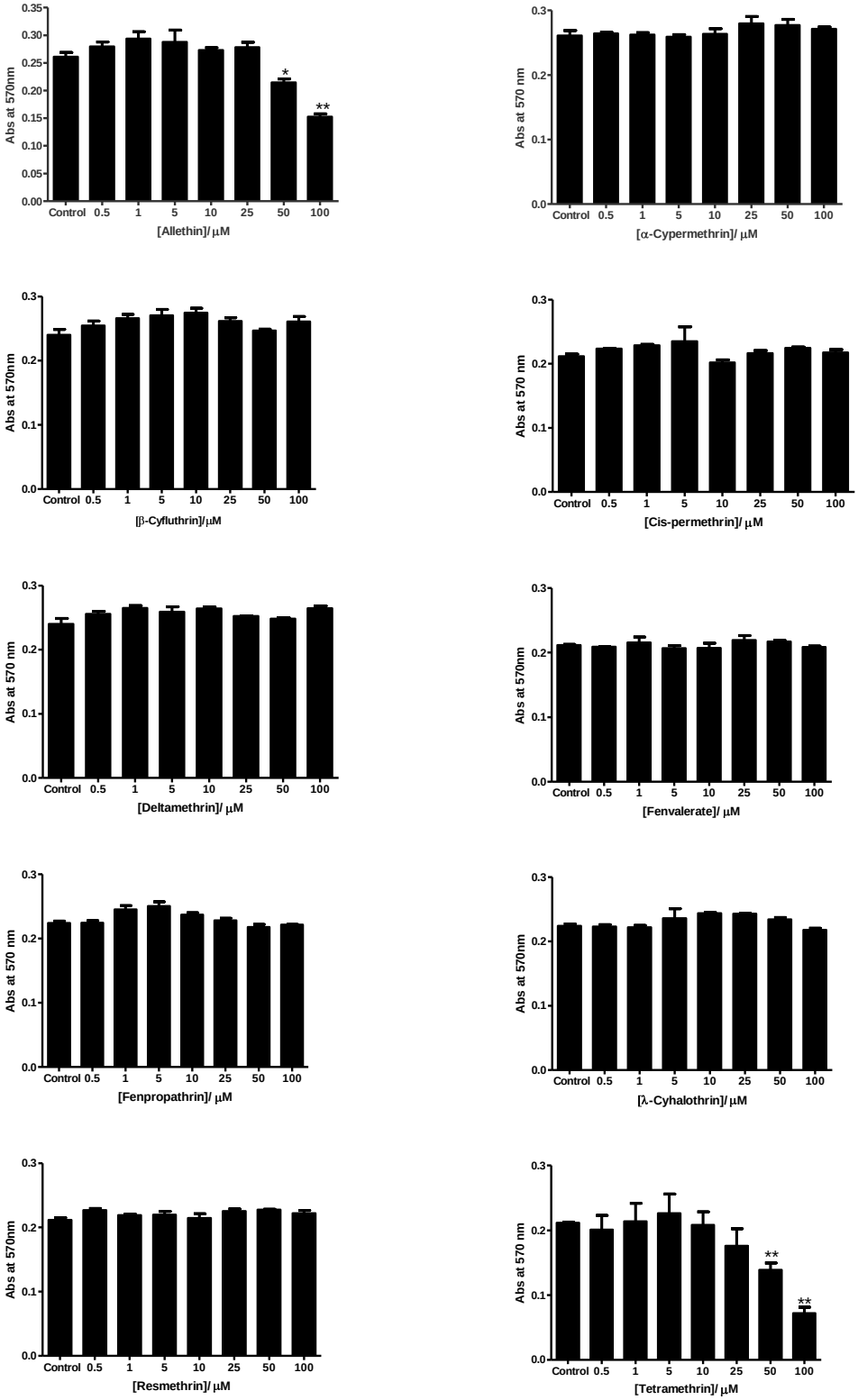

Figure 6. **Dose-dependent cytotoxicity of 10 pyrethroids on SK-N-SH cells.** The experimental design is similar to that described in Figure 5, except that the wells were initially seeded with $2x10^4$ SK-N-SH cells/well.

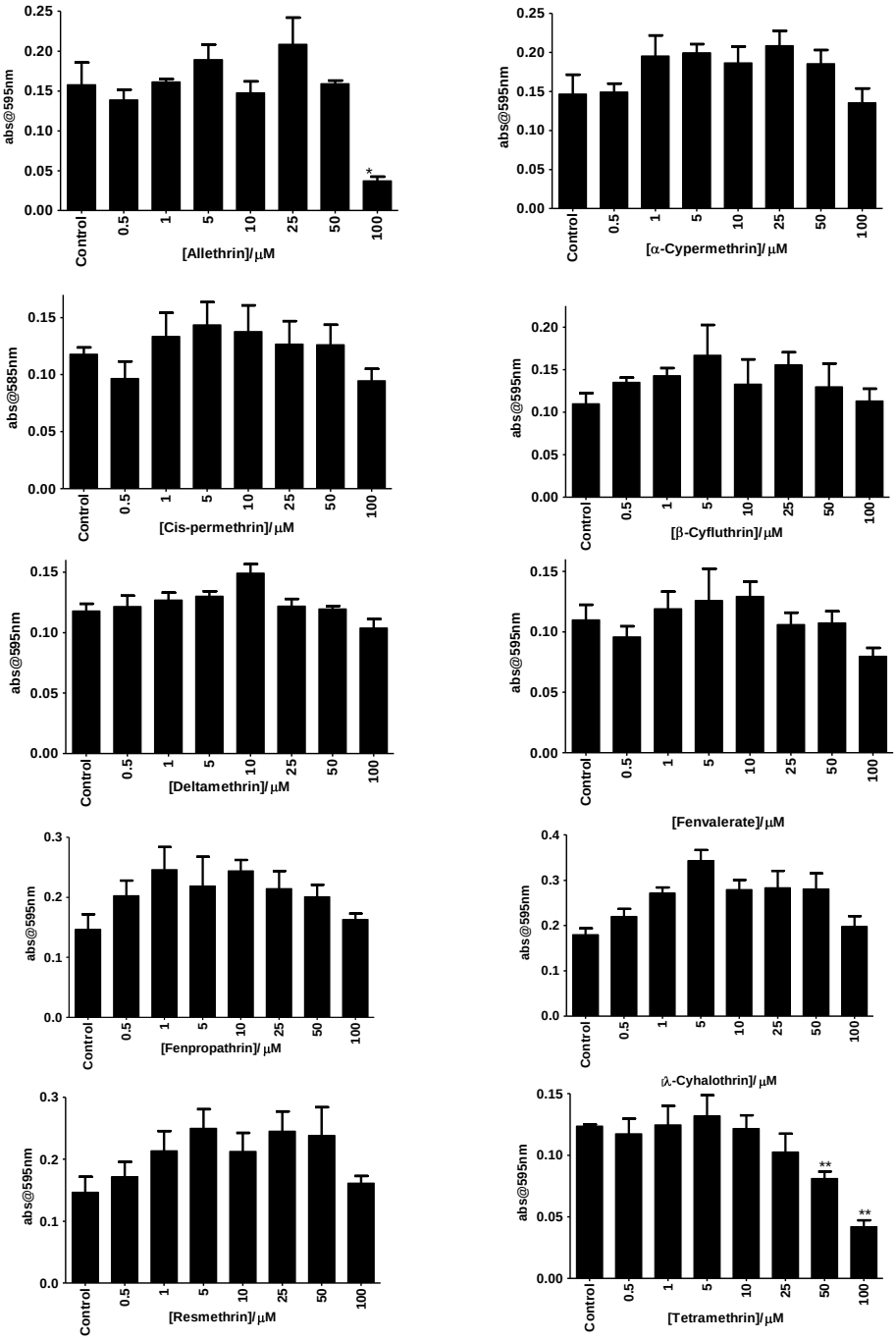

Observations and Results

Treatment of SH-SY5Y cells and SK-N-SH cells with α-cypermethrin, β-cyfluthrin, cis-permethrin, deltamethrin, fenpropathrin, fenvalerate, λ-cyhalothrin, and resmethrin over the concentration range 0.5-100 µM for 24 h produced no evidence of cytotoxicity. However, treatment of SH-SY5Y cells with 50 µM allethrin and 50 µM tetramethrin was cytotoxic (Figure 5). SK-N-SH cells were also sensitive to these compounds, with 100 µM allethrin and 50 µM tetramethrin causing cytotoxicity (Figure 6). Therefore the appropriate concentrations of test compounds for further studies were 10µM for tetramethrin, 25 µM for allethrin and 100 µM for the other eight compounds.

Functional effects

The critical neurological effects of pyrethroids relevant to cumulative risk assessment are functional rather than morphological changes. Hence, the effects of pyrethroids on relevant functional effects in the cells were evaluated. Basal and potassium stimulated release of ^{3}H-noradrenline (Seyedi et al., 2005) (Figure 7) and the uptake of 3-O-methyl-d-[1-^{3}H]glucose (^{3}H-3-OMG) by cells (Figure 8) treated with vehicle control and pyrethroids at the concentrations determined to be non-cytotoxic in preliminary studies (i.e. 10µM for tetramethrin, 25 µM for allethrin and 100µM for the other eight compounds) were investigated.

Figure 7. The effect of pyrethroids on ^{3}H-noradrenaline release. Basal and potassium-stimulated noradrenaline release was measured in SH-SY5Y, SK-N-SH and HFF-1 cells and the effect of 10 different pyrethroids determined under conditions described in experimental procedures. Each bar represents the mean and SEM from three separate experiments (each performed in triplicate). Statistically significant differences in ^{3}H-noradrenaline release between vehicle-treated control and pyrethroid treated cells in each respective are indicated (*p<0.05, Student's t-test).

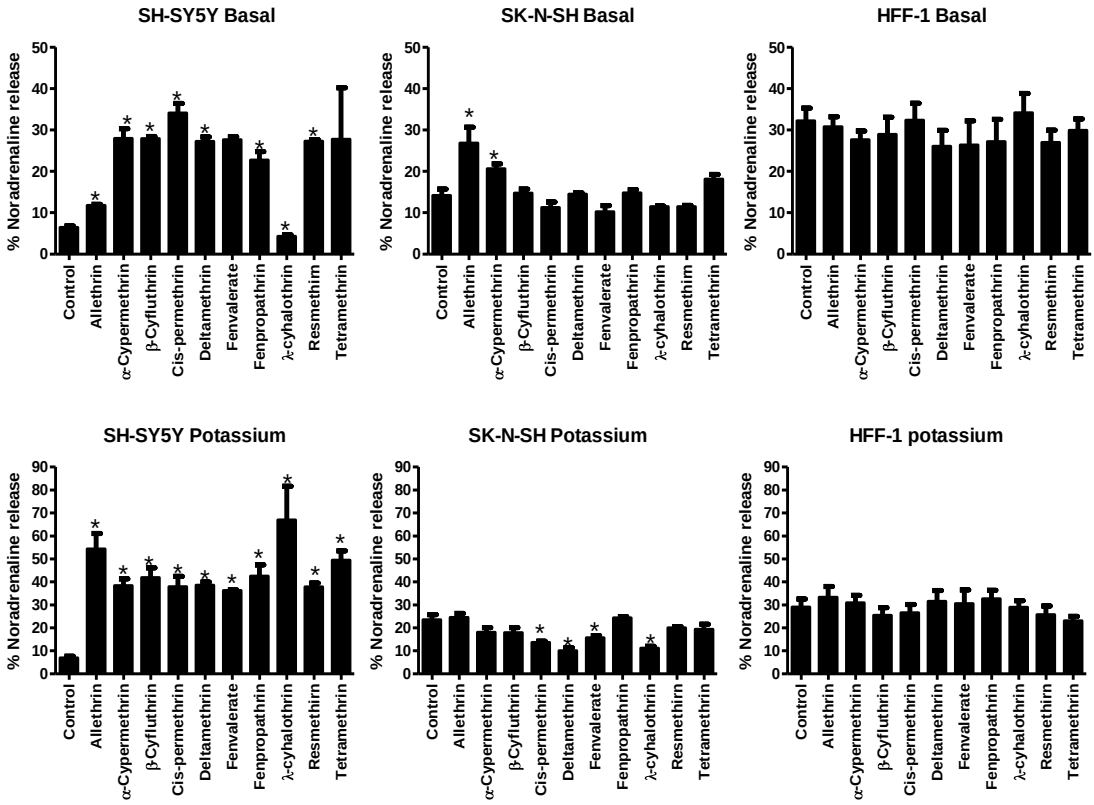

In SH-SY5Y cells noradrenaline release was affected by all of the pyrethroids tested. All of the compounds caused an increase in both basal and potassium-stimulated release with the exception of tetramethrin which did not show a significant increase and λ-cyhalothrin which caused a decrease in basal release (Figure 7). The effect on SK-N-SH cells was quite modest. Most of the compounds had little or no effect on basal release; only allethin and α-cypermethrin caused an increase in basal release (Figure 7). Potassium-stimulated release was inhibited by treatment with cis-permethrin, deltamethrin, fenvalerate and λ-cyhalothrin, although the magnitude of the change was relatively small. No significant effects were found on either basal or potassium-stimulated release by treatment of HFF-1 cells with any of the compounds (Figure 7).

Carbazemepine caused a statistically significant 50% reduction in glucose uptake in SH-SY5Y cells (Figure 8); this is consistent with previous findings (Mannerstrom and Tahti, 2004). These authors attributed the reduction in glucose uptake to blockage of sodium channels leading to a reduction in the frequency of sustained repetitive firing of action potentials, reduced ion transport, energy demand and glucose uptake. However in this current work using SH-SY5Y cells none of the pyrethroids caused a reduction in glucose uptake (Figure 8) suggesting that they did not affect the sodium channels in the same way as carbazemepine. SK-N-SH cells and HFF-1 cells appeared unresponsive to effects on the sodium channel or other pathways such that glucose uptake was not affected by either carbazemepine or any of the pyrethroids (Figure 8).

Figure 8. The effect of pyrethroids on glucose uptake. Uptake of 3-O-methyl-d-[1-^{3}H] glucose was measured in SH-SY5Y, SK-N-SH and HFF-1 cells and the effect of 10 different pyrethroids determined under conditions described in experimental procedures. Carbazemepine was also included as a positive control. Each bar represents the mean and SEM from three separate experiments (each performed in triplicate). Statistically significant differences in glucose uptake between vehicle-treated control and pyrethroid treated cells in each respective are indicated (**p<0.01; by student's t test).

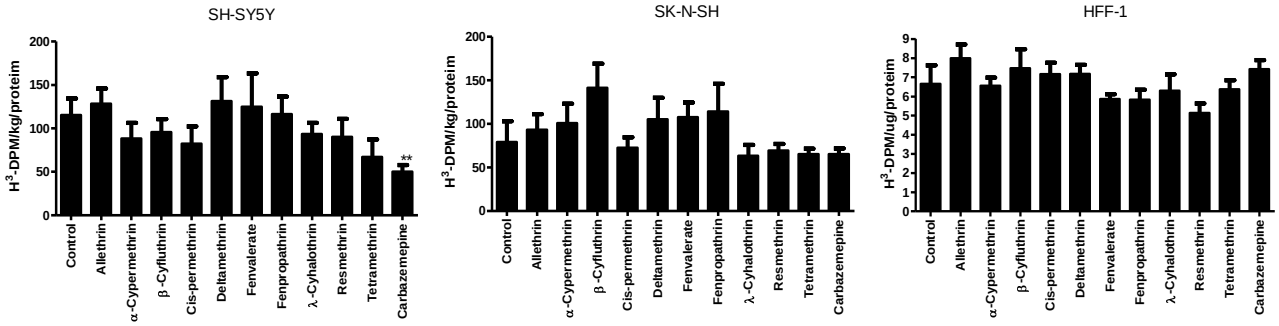

Objective 02: SELDI-TOF mass spectrometry analysis

Suitable non-cytotoxic concentrations of the test compounds were established in objective 01; these were 100 μM for each of the pyrethroids, except for allethrin and tetramethrin, which were 25 μM and 10 μM, respectively. These concentrations were used to treat cells for 24 h and the effect on intracellular protein profiles determined using SELDI TOF MS.

Initial experiments were performed to optimise the conditions for SELDI TOF MS using homogenates prepared from SH-SY5Y cells treated with allethrin, fenvalerate, or vehicle control. SELDI TOF MS was performed using ProteinChips with different surface chemistries, i.e. H50 (hydrophobic), SAX2 (strong anion exchange) and CM10 (weak cation exchange) ProteinChips. Application of samples onto the H50 ProteinChip produced only very low intensity ions, on the SAX2 ProteinChip a limited number of ions were detected, whereas use of the CM10 ProteinChip resulted in many peaks representing ~50 ions (Figure 9). The effect of varying the amount of protein loaded onto the surface was examined and it was found that for most ions a loading of 1 μg was appropriate (Figure 9). Also, the effect of varying the pH of the binding buffer was investigated and here it was found that a pH of 4 resulted in the most protein ion peaks being detected (Figure 9). Therefore, the final conditions for analysing the samples using SELDI TOF MS were CM10 (weak anion-exchange) ProteinChips loaded with 1 μg protein per spot in a pH4 binding buffer; these conditions were found to give the most and informative data. The same conditions were applied for the analysis of SK-N-SH and HFF-1 cells and in both cases informative spectra were achieved under these conditions (Figure 10). Under these conditions, reproducibility assessed as the coefficient of variation (CV) of the intensity of peaks was typically 12%.

In previous work carried out in our laboratory using MCF-7 cells we were able to establish that some of the ions in the spectra were due to core histone proteins (Zhu et al, 2009). Here again, it was found that a number of the ions were from histones H2A, H2B, H3 and H4, with both single and double charged ions being detected (Figure 10; Table 1).

Figure 9. Optimisation of SELDI-TOF MS conditions. (A). The effect of using ProteinChips with different surface chemistries. SH-SY5Y cell homogenate (1 µg/spot) was applied to H50 (hydrophobic), SAX2 (anion exchange) and CM10 (cation exchange) ProteinChip. The resultant spectra indicate that application to the CM10 ProteinChip produced a rich spectrum comprising many ions, whereas relatively few ions were detected using the other types of ProteinChip. (B). The effect of pH on the protein profiles was examined. Spectra of fenvalerate-treated SH-SY5Y cell homogenate (1 µg/spot) were produced on CM10 ProteinChip arrays using 0.1M sodium acetate (pH 3, 4, 6 and 8) and 0.1% triton X100 in the binding buffer. Many similar protein ions could be detected at each of the pHs tested, although at pH 4 the intensity of the peaks was highest and number greatest. This is particularly evident in the m/z range of 6000-14000.Different pH conditions (C). Similar conditions were applied except the amount of protein loaded was varied. Maximum ion intensity of most ions was achieved by applying 1 µg protein.

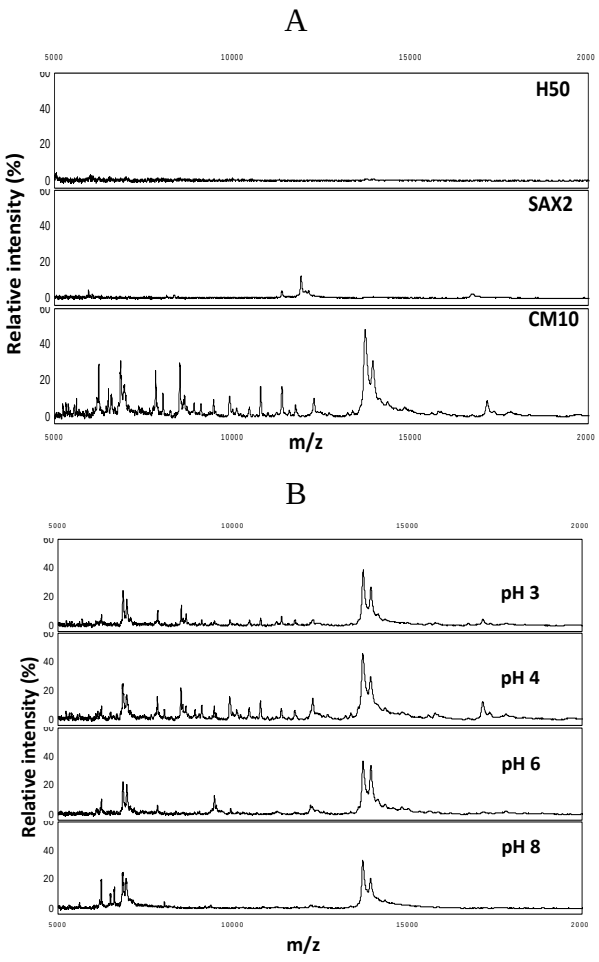

Figure 10. Typical SELDI TOF MS protein profiles for SH-SY5Y, SK-N-SH and HFF-1 cells. The profiles were obtained using optimal conditions (pH 4 buffer, 0.1 M sodium acetate, CM10 ProteinChips and a loading of 1μg of protein/spot). Protein profiles are compared with those of purified calf thymus histones.

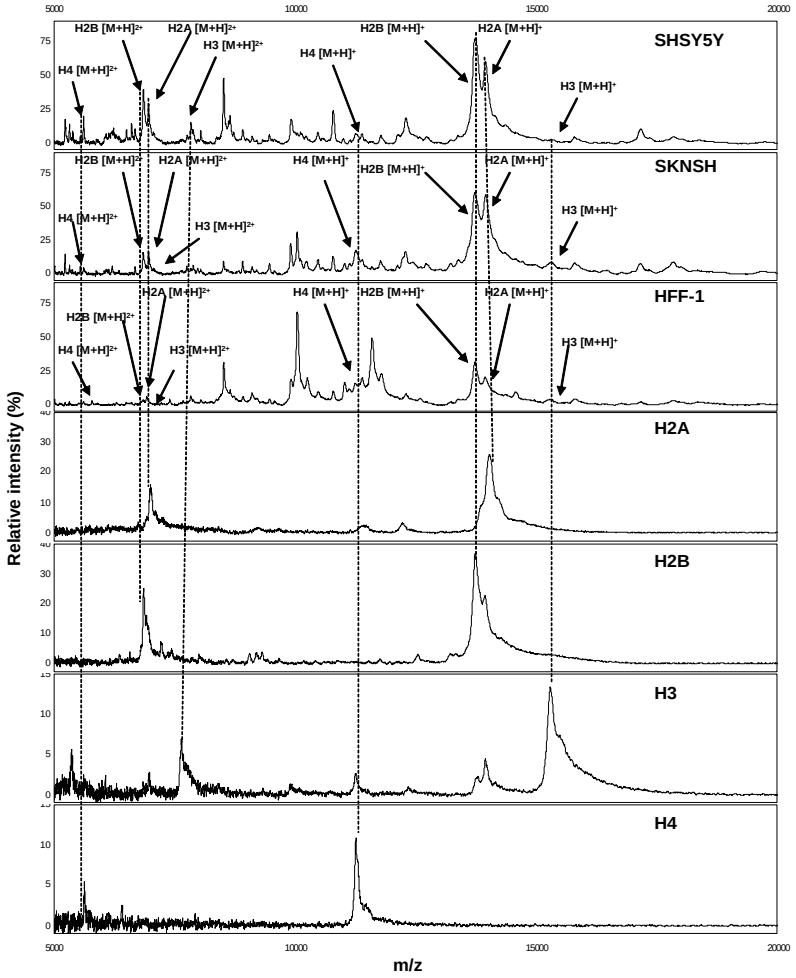

Table 1. Characteristics of purified histone proteins and histones detected in SH-SY5Y, SK-N-SH and HFF-1 cells.

Protein profile	m/z	Peak identification
H2A	13986,6994	-
H2B	13722, 6852	-
H3	15276, 7631	
H4	11246, 5623	-
SH-SY5Y	13943$[M+H]^+$, 6960$[M+H]^{2+}$ 13726$[M+H]^+$, 6854$[M+H]^{2+}$ 15294$[M+H]^+$, 7660$[M+H]^{2+}$, 11378$[M+H]^+$, 5613$[M+H]^{2+}$	H2A H2B H3 H4
SK-N-SH	13930$[M+H]^+$, 6955$[M+H]^{2+}$ 13716$[M+H]^+$, 6842$[M+H]^{2+}$ 15278$[M+H]^+$,7666$[M+H]^{2+}$, 11266$[M+H]^+$,5609$[M+H]^{2+}$	H2A H2B H3 H4
HFF-1	13933$[M+H]^+$, 6933 13717$[M+H]^+$, 6841$[M+H]^{2+}$ 15276$[M+H]^+$, 7668$[M+H]^{2+}$ 11243$[M+H]^+$,5607$[M+H]^{2+}$	H2A H2B H3 H4

Effect of pyrethroids on SH-SY5Y cells

SH-SY5Y cells were treated with 10 different pyrethroids as well as the vehicle control in 5 replicate cultures each and the entire experiment was repeated on two separate occasions. The SELDI-TOF MS data from both experiments were combined and the intensity values of 50 ions in the spectra compared and analysed statistically.

Univariate analysis

A simple univariate analysis approach was attempted by comparing the relative intensities of the ions in the vehicle control group with those in each of the pyrethroid groups. Although a number of statistically significant differences were apparent they reflected rather modest changes in intensities and did not indicate any consistent effect. For example, although the relative levels of m/z 13986 (histone H2A) were raised in cells treated with allethrin and α-cypermethrin the difference was small (~20%) and was not evident for any of the other compounds (Figure 11). This approach to the analysis was not informative.

Figure 11. Relative intensity of m/z 13986 (histone H2A) in the SELDI TOF MS spectra of SH-SY5Y cells treated with pyrethroids. The filled bars indicate mean levels (± SE). * p<0.05, Student's t-test.

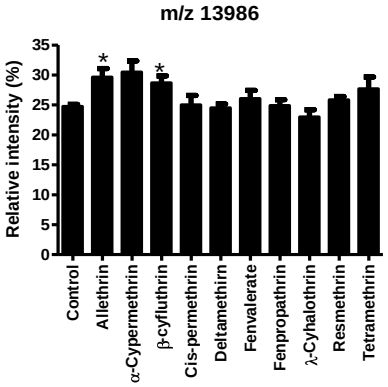

Unsupervised multivariate data analysis: PCA of pyrethroid-treated SH-SY5Y cells

Principal component analysis (PCA) is an unsupervised multivariate mathematical procedure that transforms a number of possibly correlated variables (in this case measurements of the intensity of detected ions) into a smaller number of uncorrelated variables called principal components. The first principal component (PC1) accounts for the most variability in the data and each succeeding component accounts for as much of the remaining variability as possible. Principal component analysis was carried out on all of the 50 ions detected in the SELDI TOF MS protein profiles for the vehicle-control and pyrethroid treated SH-SY5Y cells to determine if patterns emerged that could be used to classify the treatment groups (which would be due to the changes in the intensities of the ions in the protein profiles due to treatment with the test compounds).

A scree plot of the contribution of the main principal components indicated that more than 65% of the variation could be accounted for by the first two principal components (Figure 12). A score plot of the distribution of the data with respect to the first 2 principal components is shown in Figure 13. However,

no distinct separation of data from different treatment groups was evident. In some cases treatment groups were clustered together (e.g. tetramethrin) but most were scattered about the axes. In the plot, the filled symbols indicate treatment groups: cis-permethrin, deltamethrin, fenvalerate, fenpropathrin and λ-cyhalothrin, most of which had increased PC1 values (and were found in later analysis to group together). However, these data alone are insufficient to draw any conclusions regarding commonality of response to treatment with the different pyrethroids. It seems probably that the relatively small variation in the intensity of the ions caused by treatment with the different pyrethroids apparent from univariate analysis underlies the inability to differentiate between treatment groups using PCA.

Figure 12. Scree plot for the PCA analysis of the entire data set for both experiments. The first two principal components described the majority of the variation in the data.

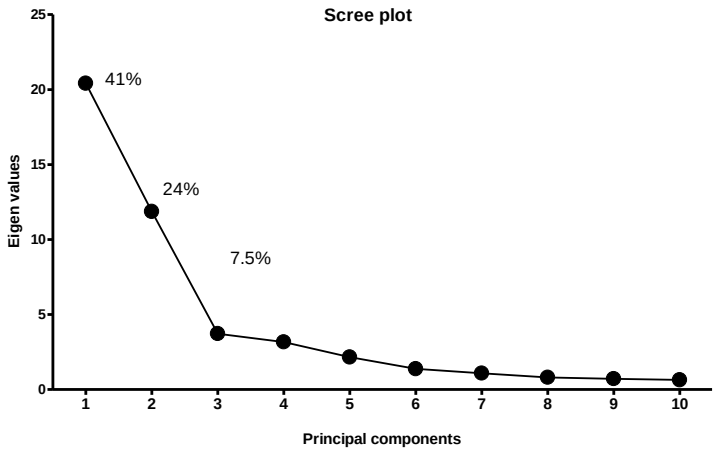

Figure 13. PCA of SELDI-TOF MS data from pyrethroid-treated SH-SY5Y cells. The data are presented as a score plot of the first two principal components (PC1and PC2) based on the intensities of all of the ions detected in the analysis. A histogram showing the 10 variables that contributed most to factors 1 and 2 is shown below.

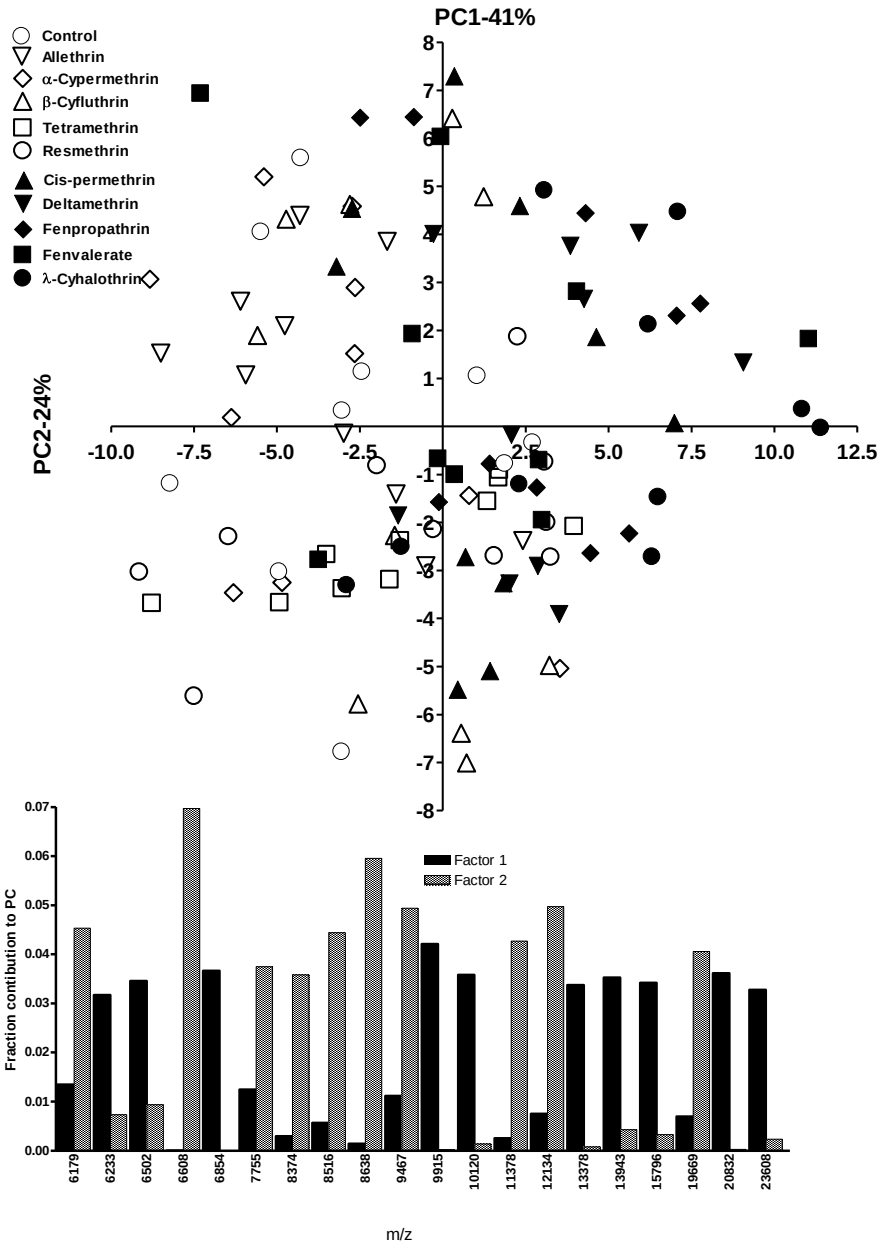

Supervised Multivariate Analysis

Stepwise linear discriminant function analysis is a supervised multivariate mathematical procedure in which variables (in this case measurements of intensity of detected ions) are systematically placed into a model that attempts to classify groups within the dataset. At each step the variable that makes the most significant contribution to the classification of the specified groups is selected. Variables that correlate with those in the model are excluded as their inclusion has no or only limited additional discriminatory power. The final model is in the form of a multivariate regression equation that ideally defines those variables that separate the supervised groups. As neither the univariate approach nor the PCA analysis gave any clues as to any possible grouping, further supervised analysis was applied in an exploratory manner by examining different putative classification groups.

(i) Classification based on two groups comprising treatment with vehicle-control and treatment with any pyrethroid.

In this analysis the effect of the different pyrethroids as a single group compared with the vehicle-control was considered. Linear forward stepwise discriminant function analysis was applied over 10 iterations (steps) which resulted in up to 98% classification. A single ion (m/z 6502) was able to correctly classify 69% of the data (Figure 14A) but on receiver operator curve (ROC) analysis produced an area under the curve (AUC) of only 74%. However, a combination of 3 protein ions produced a model that correctly classified 93% of the data (Figure 14A and B). A multiple regression equation based on the coefficients determined from the discriminant function analysis was used to calculate values for each sample and the results are shown in Figures 14C and 14D. The ROC-AUC was 96% (Figure 14E), indicating that this model performed well. When the results from the two independent experiments were analysed separately classifications of 95% and 91% were obtaining using the 3 protein ions. Thus, it is reasonable to deduce that all of the pyrethroids had an effect on the SH-SY5Y cells that resulted in a common alteration of their protein profiles.

Figure 14. **Classification of the effect of 10 pyrethroids as a single group compared with vehicle control.** Using a forward stepwise approach a discriminant function analysis model was built by inclusion of informative data from a series of ions as indicated in (A). The resultant effect on classification at each step is illustrated in (B). A combination of 3 proteins with ions m/z = 6502, 11378, 6138 produced a model that correctly classified 93% of the data. Regression coefficients calculated from discriminant function analysis of this combination were used to produce a multiple regression equation (y = *m1*x1+ *m2*x2 + m3x3 +c, where y = relative intensity, *x1* =intensity of m/z 6502 ion, *x2* = intensity of m/z 11378 ion, x3 = intensity of m/z 6138 ion, *m1* = 1.230, *m2 -0.818*, m3= 0.753 and c = -7.632) which describes the relationship. (C) Calculated values for different sample groups. (D) Comparative values in the two groups with the dotted line indicating a cut-off value that correctly classifies 93% of samples. (E) The performance of this classification summarised as a ROC; an AUC of 96% was achieved.

A

Steps	%	m/z
1	69	6502
2	77	11378
3	93	6138
4	92	15796
5	94	6078
6	93	8909
7	96	8516
8	96	10035
9	97	10120
10	98	20832

B

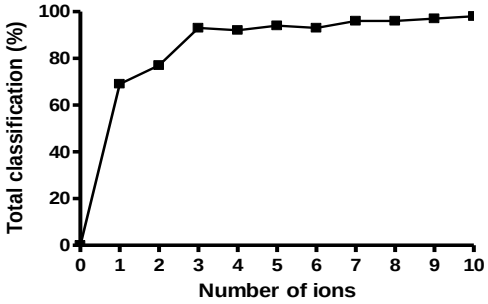

C

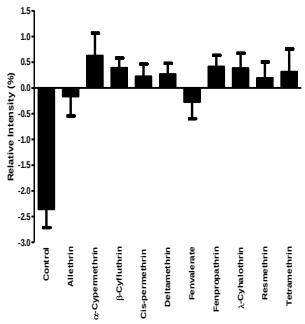

D

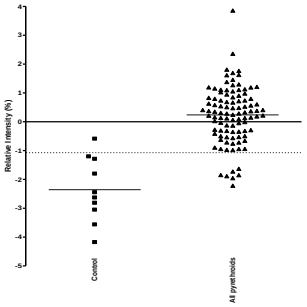

E

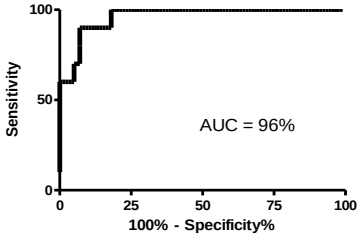

(ii) Classification based on type I and type II pyrethroids.

The pyrethroids were grouped as type I (allethrin, cis-permethrin, resmethrin and tetramethrin) and type II (α-cypermethrin, β-cyfluthrin, deltamethrin, fenvalerate, fenpropathrin, λ-cyhalothrin) and stepwise linear discriminant function analysis applied to the data. It was found that a single protein ion with m/z 8638 was able to correctly classify only 65% of the data (Figure 15A). The regression coefficient calculated from discriminant function analysis with this variable was used to produce a regression equation to describe the relationship and the values calculated for each treatment group are shown in Figure 15C and for individual samples in Figure 15D to show the distribution of the data. The ROC-AUC was 65% (Figure 15E), indicating that this model did not perform well. When the results from the two independent experiments were analysed separately, in one no classification could be obtained and in the other the same 3 protein ions were not included in the model. Thus, it is reasonable to deduce from this that the pyrethroids cannot be classified as type I and type II based on alterations in the protein profiles of SH-SY5Y cells.

The addition of data from other ions into the model produced only slightly improved classification, but with no clear progress to forming a model capable of distinguishing between the pyrethroids on this basis (see table in Figure 15A). A combination of 4 protein ions produced a model that correctly classified only 70% of the data and the ROC-AUC was just 70%.

Figure 15. Classification of the effect of type I and type II pyrethroids on protein profiles. Classification based on assignment as a type I or type II pyrethroid was assessed using forward stepwise discriminant function analysis. (A) Data using the intensity of the m/z = 8638 ion produced a model that correctly classified 65% of the data. (B) However, this was not improved greatly by incorporating data from other ions, indeed including ions at steps 3 and 4 was only possible using manual settings. (C) The single ion model based on linear regression for intensity of m/z 8638 failed to distinguish the effect of groups of type I and type II compounds (D) nor individual samples (broken line indicates optimal cut-off). (E) ROC-AUC was 65%. (F,G) Similarly, multiple regression analysis using 2 ions also failed to distinguish between the effect of groups of type I and type II pyrethroids. (H) ROC-AUC was 78%.

A

Steps	%	m/z
1	65	8638
2	64	7838
3*	65	15796
4*	70	20832

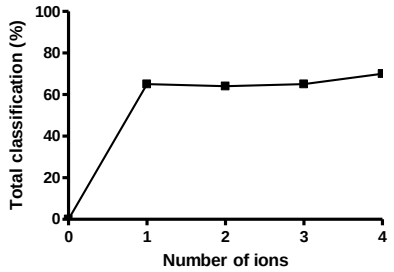

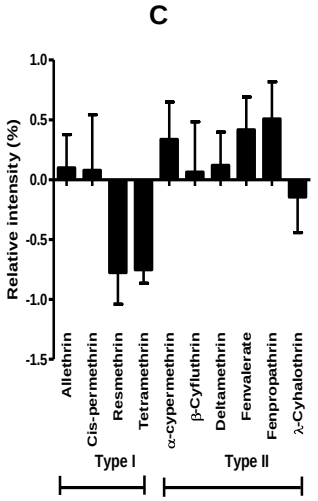

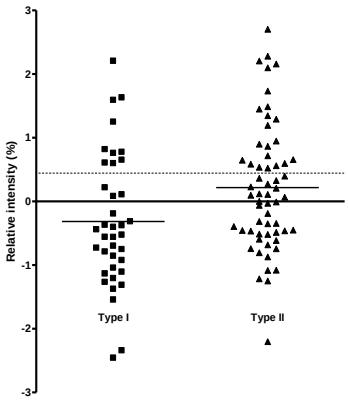

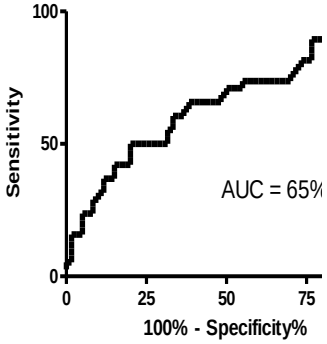

1 ion

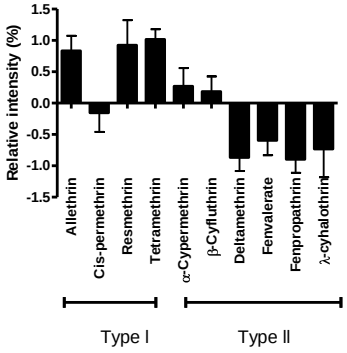

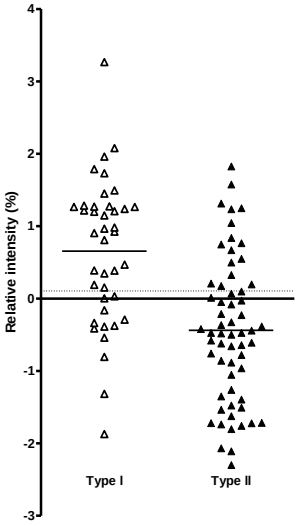

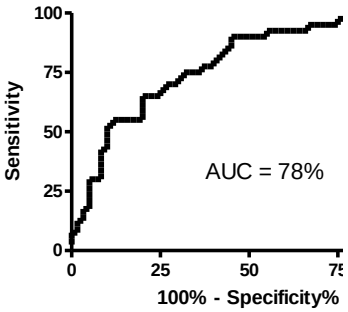

(iii) Development of a novel classification model. Presentation of SELDI-TOF MS data in the form of a so-called volcano plot is useful for obtaining an overview of the dataset and for identifying any outliers. In such plots data for each ion are compared with respect to a control experiment and the difference is represented as fold change and statistical significance. Fold change is plotted on a $\log_2$ scale, so that increased and decreased levels appear relative to a centrally place ordinate. Statistical significance (p-value) is plotted on a negative $\log_{10}$ scale so that data with greater statistical significance are plotted furthest from the abscissa. The fold change indicates biological impact of the change and the statistical significance the certainty of the change (Cui and Churchill, 2003). A series of volcano plots has been produced to illustrate the effect of treatment of each pyrethroid in comparison with vehicle control treated cells.

Interpretation of the data is based on consideration of the distribution of data points and deviation from the origin. In those cases where treatment has little or no effect then one would expect to see data symmetrically distributed about a mean $\log_2$ value of zero fold change. As data points deviate further from the origin, they increase in their statistical significance values. The pattern shown for data obtained following the treatment of SH-SY5Y cells with allethrin is typical (Figure 16A). There is only a small amount of variation in the levels of the intensity of the protein ions, with none outside the $\log_2$ range of -0.25 to 0.25 (equivalent to 0.8-1.2 fold difference) and only a few with p-values of <0.05. Similar profiles are evident for SH-SY5Y cells treated with α–cypermethrin, β–cyfluthrin, resmethrin and tetramethrin (Figure 16A, upper plots). However, it was notable that plots of data produced from cells treated with λ-cyhalothrin, deltamethrin, fenvalerate, fenpropathrin and *cis*-permethrin were quite different (Figure 16A, lower plots). For these 5 compounds the data is clearly skewed to the left indicating that the levels of the majority of the protein ions were decreased on treatment. This resulted in an increased number of data points with statistical significance $p<0.05$, and a larger number outside the lower fold-variation range indicated, although the values were still within $\log_2$ -0.5 (0.7 fold) of the control. Seven (m/z = 6502, 9915, 13378, 13943, 15796, 20832 and 23608) out of nine of the ions indicated for λ-cyhalothrin, deltamethrin, fenvalerate, fenpropathrin and *cis*-permethrin were amongst those that contributed to PC1 (Figure 13). It is evident that a number of ions show a similar tendency of down regulation in cells treated with λ-cyhalothrin, deltamethrin, fenvalerate, fenpropathrin and *cis*-permethrin and it was apparent that treatment with these compounds caused a coordinated change in the levels of many protein ions. This observation was evident in two independently performed experiments (Figures 16B and C). The coincident effect is reflected in the correlation that exists between the intensity values of many of the protein ions (Table 2; Figure 17). As the data are well correlated but the magnitude of change is small it proved difficult for PCA to identify specific protein ions that adequately represent the entirety of the data. Similarly, analysis of the levels of individual protein ions by univariate statistical analysis proved uninformative due to the small amount of variation between the samples. Thus, the effect of the pyrethroids on the protein ions detected by SELDI-TOF MS is small but extensive. On the basis of the changes in the protein ion profiles it is possible to define two groups, which we call here group A, where no observable effect on the profile was found and group B where an extensive change in the protein profile was observed (Table 3). In an attempt to quantify the difference, a value representing the average of fold changes of all ions in the spectra was calculated and compared between the treatment groups. There was no statistically significant differences within the treatment group A (allethrin, α–cypermethrin, β–cyfluthrin, resmethrin and tetramethrin) and in most cases the levels in members of group B (deltamethrin, fenvalerate, fenpropathrin, and *cis*-permethrin) were significantly higher (Figure 18).

Figure 16. Volcano plots showing the effect of treatment of SH-SY5Y cells with 10 pyrethroid compounds. For each protein ion detected the average intensity following treatment with each pyrethroid is expressed as a ratio of the intensity in vehicle-control treated samples and represented as fold change (abscissa) and statistical significance (ordinate). Dotted lines indicate fold changes of 0.8 and 1.2 and a significant level 0.05 (Student's t-test). Overall the majority of the data where within these fold changes and significance levels. However, treatment with those pyrethroids shown in the lower panel (group B) showed a tendency for down regulation of a number of ions, some of which are indicated by arrows. Panel (A) shows the data from two experimental repeats combined. Panels (B) and (C) show the data for the individual independently performed experiments.

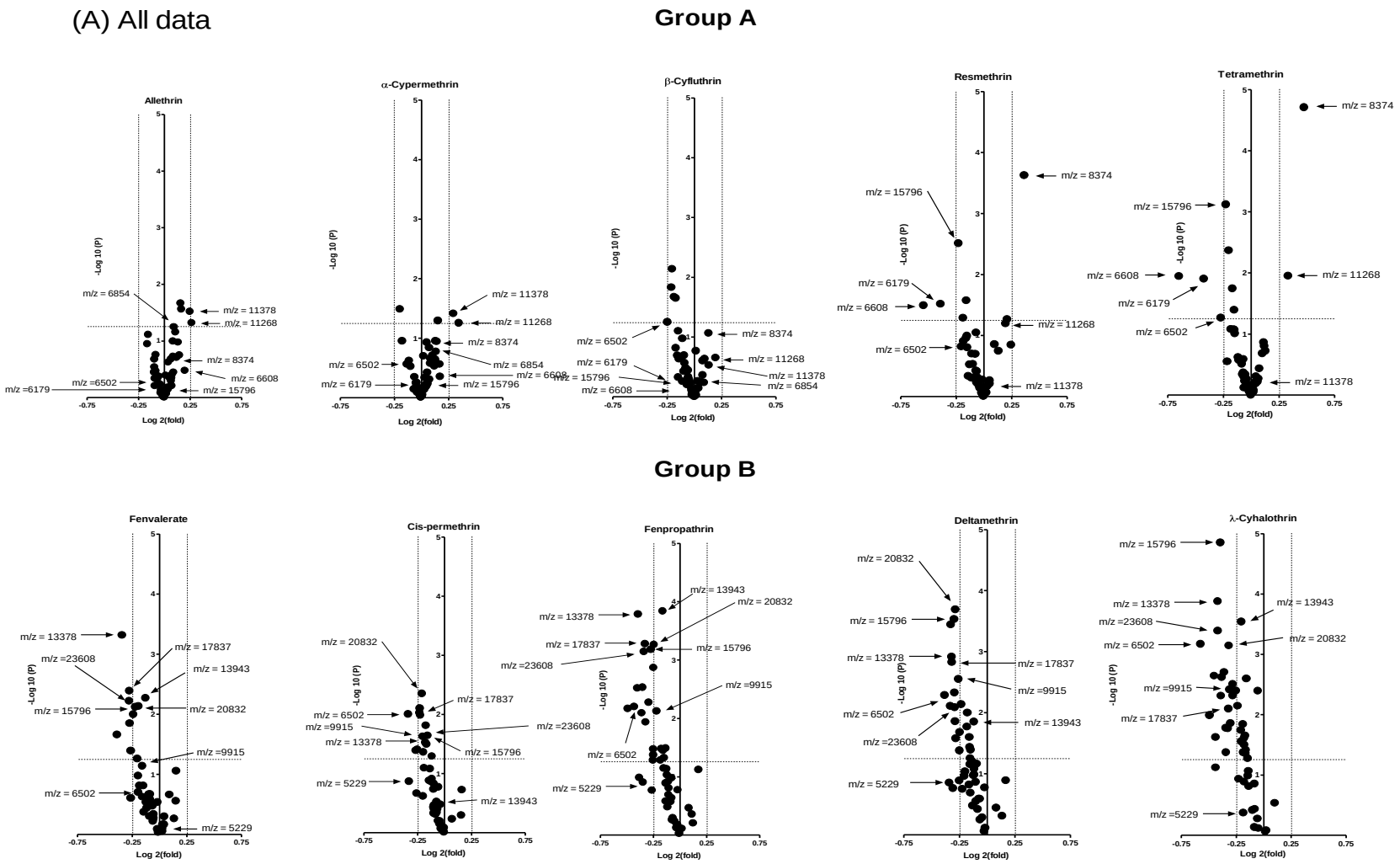

(B) Experiment 1

Group A

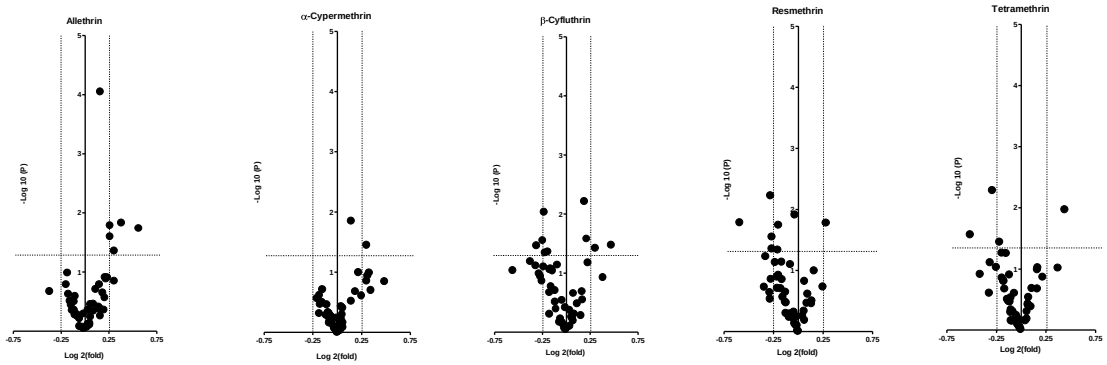

Group B

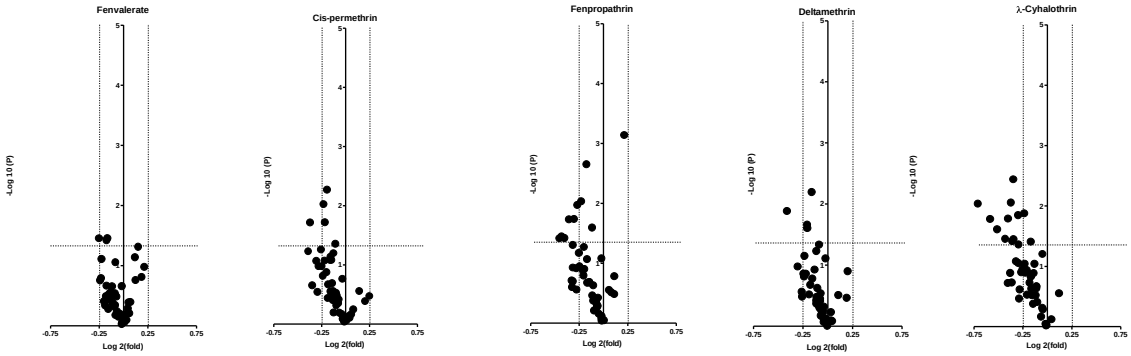

(C) Experiment 2

Group A

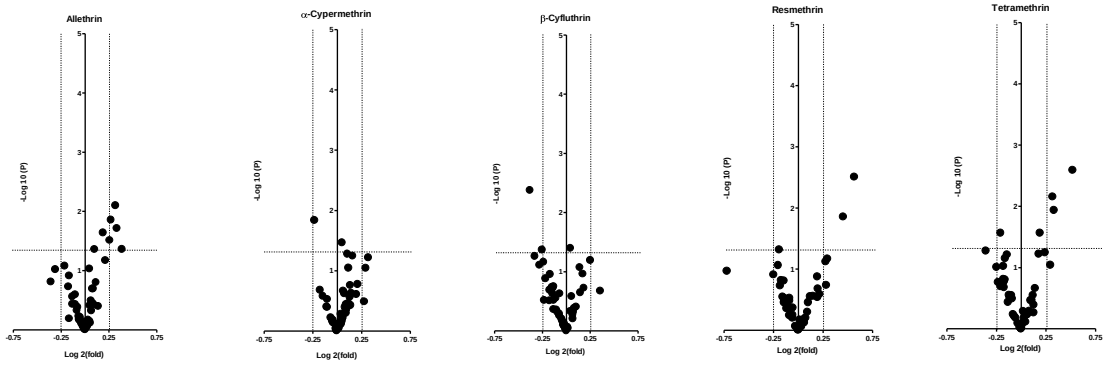

Group B

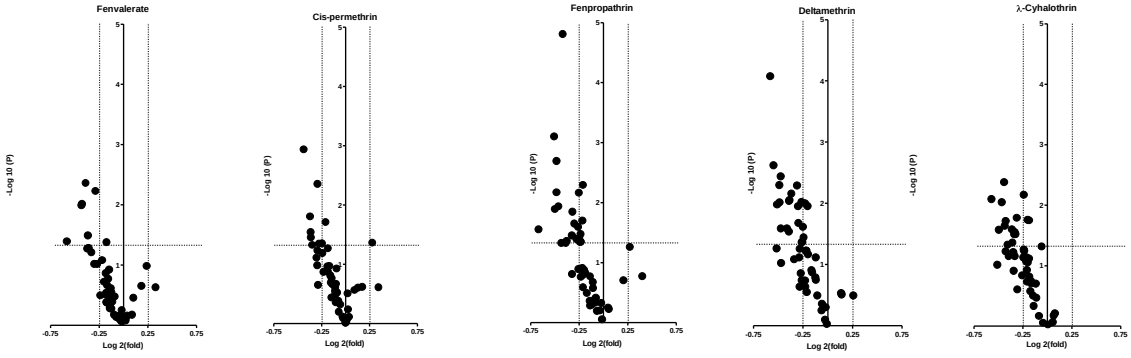

Table 2. Correlation matrix showing the relationship between ions in the SELDI-TOF MS spectra. The 20 ions that contribute to the first two principal components (PC1: grey boxes; PC2: clear boxes) of the PCA score plot (Figure 15) were selected and the correlation coefficients between them indicated. Those with a value of 0.7 or greater are highlighted (red).

m/z	6179	6233	6502	6608	6854	7755	8374	8516	8638	9467	9914	10120	11378	12134	13378	13943	14796	19669	20832	23608
6179	-	0.66	0.81	0.73	0.47	-0.31	-0.48	0.54	0.73	0.79	0.4	0.31	0.68	-0.37	0.43	0.25	0.6	0.76	0.52	0.37
6233	0.66	-	0.84	0.25	0.65	0.31	0.01	0.51	0.29	0.66	0.71	0.57	0.37	0.17	0.65	0.58	0.67	0.47	0.68	0.63
6502	0.81	0.84	-	0.29	0.7	0.14	-0.14	0.4	0.39	0.69	0.72	0.65	0.4	0.05	0.69	0.56	0.73	0.62	0.8	0.7
6608	0.73	0.25	0.29	-	-0.02	-0.58	-0.71	0.65	0.8	0.61	-0.09	-0.22	0.76	-0.66	-0.03	-0.17	0.24	0.58	-0.04	-0.14
6854	0.47	0.65	0.7	-0.02	-	0.44	0.3	0.32	0.19	0.38	0.76	0.67	0.14	0.23	0.66	0.73	0.67	0.16	0.63	0.55
7755	-0.31	0.31	0.14	-0.58	0.44	-	0.54	-0.16	-0.48	-0.3	0.51	0.44	-0.33	0.76	0.43	0.61	0.29	-0.42	0.23	0.42
8374	-0.48	0.01	-0.14	-0.71	0.3	0.54	-	-0.2	-0.51	-0.28	0.3	0.38	-0.43	0.6	0.05	0.26	-0.11	-0.43	0.18	0.18
8516	0.54	0.51	0.4	0.65	0.32	-0.16	-0.2	-	0.67	0.72	0.32	0.22	0.56	-0.36	0.13	0.13	0.38	0.47	0.22	0.04
8638	0.73	0.29	0.39	0.8	0.19	-0.48	-0.51	0.67	-	0.69	0.14	0.09	0.57	-0.62	-0.04	-0.09	0.28	0.71	0.17	-0.05
9467	0.79	0.66	0.69	0.61	0.38	-0.3	-0.28	0.72	0.69	-	0.39	0.34	0.62	-0.38	0.25	0.19	0.42	0.77	0.53	0.28
9914	0.4	0.71	0.72	-0.09	0.76	0.51	0.3	0.32	0.14	0.39	-	0.89	0.13	0.38	0.71	0.75	0.78	0.33	0.8	0.74
10120	0.31	0.57	0.65	-0.22	0.67	0.44	0.38	0.22	0.09	0.34	0.89	-	0.08	0.39	0.65	0.72	0.64	0.33	0.82	0.71
11378	0.68	0.37	0.4	0.76	0.14	-0.33	-0.43	0.56	0.57	0.62	0.13	0.08	-	-0.4	0.22	0.12	0.38	0.56	0.22	0.11
12134	-0.37	0.17	0.05	-0.66	0.23	0.76	0.6	-0.36	-0.62	-0.38	0.38	0.39	-0.4	-	0.46	0.55	0.25	-0.36	0.26	0.5
13378	0.43	0.65	0.69	-0.03	0.66	0.43	0.05	0.13	-0.04	0.25	0.71	0.65	0.22	0.46	-	0.88	0.84	0.22	0.74	0.85
13943	0.25	0.58	0.56	-0.17	0.73	0.61	0.26	0.13	-0.09	0.19	0.75	0.72	0.12	0.55	0.88	-	0.76	0.08	0.66	0.76
14796	0.6	0.67	0.73	0.24	0.67	0.29	-0.11	0.38	0.28	0.42	0.78	0.64	0.38	0.25	0.84	0.76	-	0.43	0.69	0.7
19669	0.76	0.47	0.62	0.58	0.16	-0.42	-0.43	0.47	0.71	0.77	0.33	0.33	0.56	-0.36	0.22	0.08	0.43	-	0.56	0.34
20832	0.52	0.68	0.8	-0.04	0.63	0.23	0.18	0.22	0.17	0.53	0.8	0.82	0.22	0.26	0.74	0.66	0.69	0.56	-	0.84
23608	0.37	0.63	0.7	-0.14	0.55	0.42	0.18	0.04	-0.05	0.28	0.74	0.71	0.11	0.5	0.85	0.76	0.7	0.34	0.84	-

Stepwise linear discriminant function analysis was then performed on the suggested classification into groups A and B (Figure 19). It was found that the major classifier was the intensity of the m/z 13378 ion. Subsequent inclusion of data from the intensity of other ions into the model improved the classification slightly although data from just two ions (m/z 13378 and 8374) appeared sufficient to describe the model giving an overall correct classification of 82%. Similar results were obtained in two separate experiments giving classification values of 72% and 86%). A multiple regression model based on the intensity of these two ions resulted in a ROC AUC of 94%, which indicates that the model performed well, although only a partial discrimination between the two groups was achieved.

Figure 17. Multiple correlations between ion intensities in the SELDI-TOF MS spectra of pyrethroid-treated SH-SY5Y cells. A correlation matrix of all ions detected in the spectra was produced and the values are summarised in the histogram. It is noticeable that the data a positively skewed indicating that the dataset contains a large number of positive correlations coefficients.

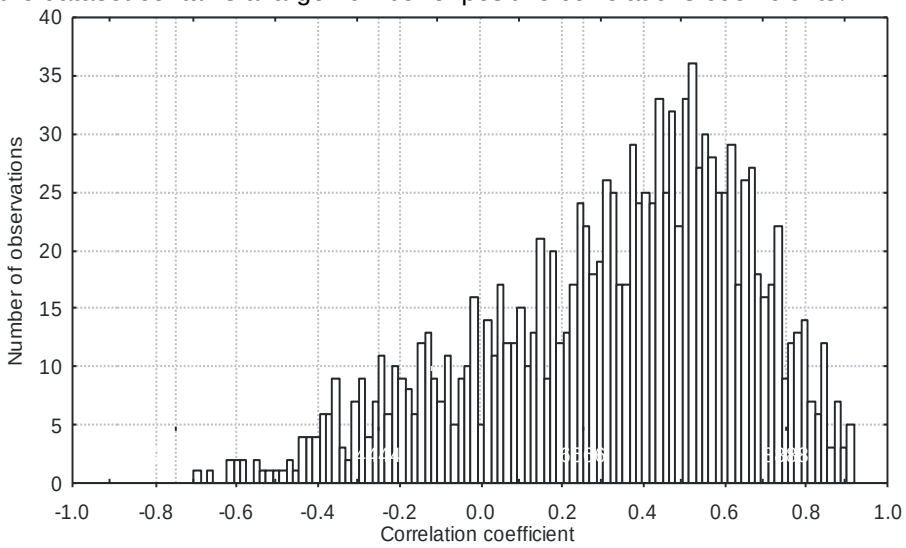

Table 3. Classicisation of pyrethroids into groups A and B in comparison to their status as type I or II compounds.

Compound	Group A/B	Type I/II
allethrin	A	I
α–cypermethrin	A	II
β–cyfluthrin	A	II
resmethrin	A	I
tetramethrin	A	I
deltamethrin	B	II
fenvalerate	B	II
fenpropathrin	B	II
cis-permethrin	B	I
λ-cyhalothrin	B	II

Figure 18. Quantification of the distribution of the intensity of ions. Mean $\log_2$(fold) values were calculated for all ions in the spectra for each compound. Statistical significant differences between the groups were determined using Tukey's multiple comparison test. There was no statistically significant differences between the treatments in group A (allethrin, α-cypermethrin, β-cyfluthrin, resmethrin and tetramethrin ($p>0.05$)), and for the majority of the treatments in group B (deltamethrin, fenvalerate, fenpropathrin and *cis*-permethrin). However in group B *cis*-permethrin and fenvalerate were statistically significant from λ-cyhalothrin ($p<0.05$). There were also statistically significant differences between groups A and B. Allethrin and α-cypermethrin were statistically different from all five of the compounds in group B ($p<0.05$) and β-cyfluthrin, resmethrin and tetramethrin were statistically different from deltamethrin, fenpropathrin and λ-cyhalothrin ($p<0.05$). However *cis*-permethrin and fenvalerate were not statistically statistically different from β-cyfluthrin, resmethrin and tetramethrin ($p>0.05$).

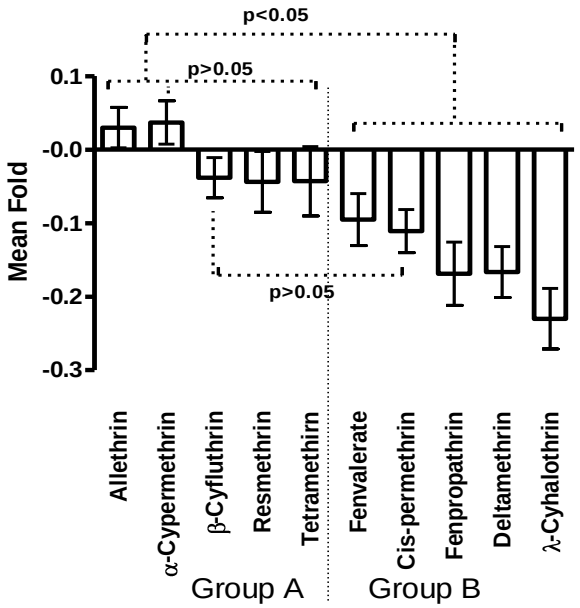

Figure 19. Classification based on the effect of group A and group B pyrethroids on protein profiles of SH-SY5Y cells. Classification based on assignment as a group A or group B pyrethroid was assessed using forward stepwise discriminant function analysis. (A) Two ions with m/z = 8374 and 13378 were sufficient to describe the classification. (B) There was no improvement to the classification by including data from additional ions. (C) Based on the regression coefficients calculated from the discriminant function analysis a multiple regression equation was deduced: y = *m1*x1+ *m2*x2 +c, where y = relative intensity, *x1 = intensity of ion m/z* 8374, *x2 = intensity of ion m/z* 13378, *m1* = 1.099, *m2* = 1.025, and c = -10.84 and the values for each group are plotted. (D) Values for individual samples with the optimal cut-off level indicated. (E) ROC analysis, with AUC 94%.

A

Steps	%	m/z
1	76	13378
2	82	8374
3	85	12713
4	82	5229

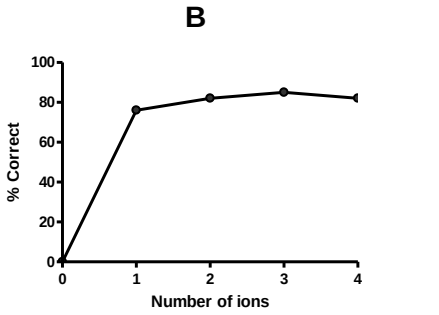

As the intensity of the m/z 13378 ion correlated with a number of other ions (Table 2), it seemed likely that many of these could substitute for m/z 13378. This was examined by replacing the data for m/z 13378 with five other correlating ions in combination with m/z 8374 (Table 4). In each case a reasonable classification resulted, albeit with slightly poorer values than for the original ion. On the other hand the m/z 8374 ion did not correlate strongly with any other ion (Table 2) and it was not possible to replace this ion in the model with any other similarly performing ion.

Table 4. The effect of replacement of the m/z 13378 with other ions on the classification of group A and B pyrethroids.

m/z	Classification in combination with m/z=8374 (%)	AUC (%)
13378	82	94
15796	82	86
9915	78	83
13943	76	86
20832	74	81
23608	76	83

Effect of pyrethroids on SK-N-SH cells

Univariate analysis

The relative intensities of 52 ions detected in the SELDI TOF MS spectra were analysed for variation in response to treatment with each of the pyrethroids tested. When analysed individually no statistical significant differences were evident between the control and any of the treatment groups ($p > 0.05$, Student's t-test).

Unsupervised data analysis

The data was subjected to PCA. A score plot of the first two principal components failed to show any particular grouping, with data from the different treatment groups (including the control) spread over all four quadrants of the plot (Figure 20). This analysis did not give any indication of a common effect of any of the treatment groups.

Figure 20. PCA score plot of SELDI TOF MS data produced following treatment of SK-N-SH cells with pyrethroids. The score plot shows the first two principal components, PC1 and PC2, and is based on the intensities of all 52 ions detected in SELDI TOF MS protein profiles of the vehicle-control and pyrethroid-treated SK-N-SH cells. A histogram showing the 10 variables that contributed most to factors 1 and 2 is shown below.

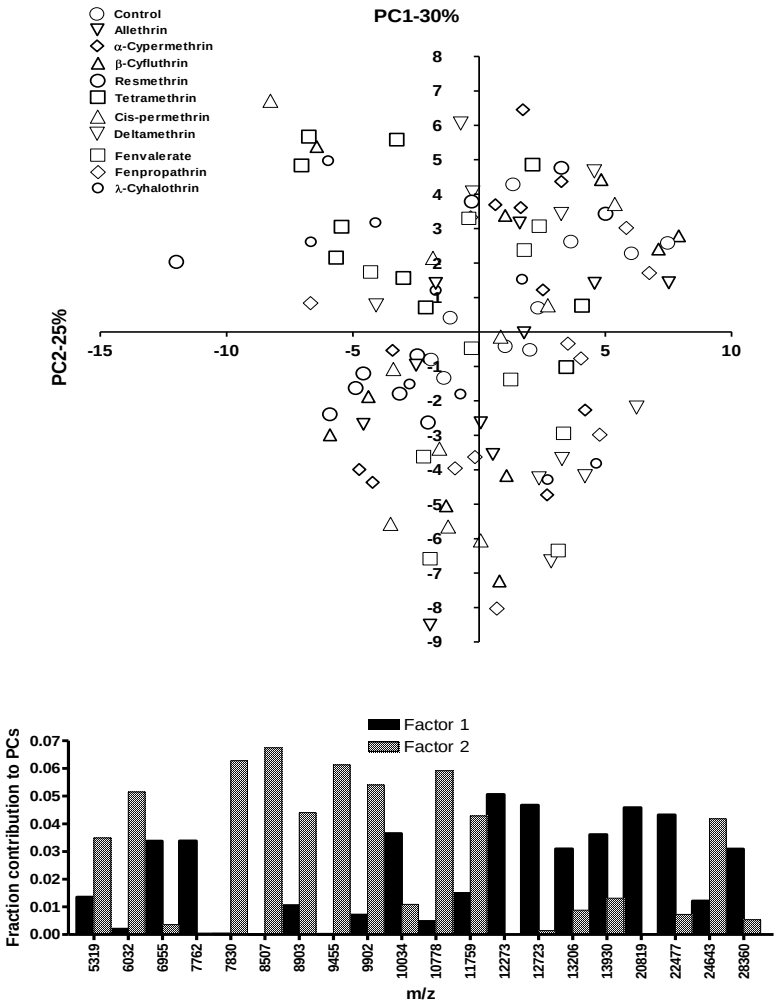

Supervised Multivariate Analysis

As the preliminary analyses were uninformative as to possible relationships between the treatment groups the same process of analysis performed for SH-SY5Y cells was also applied to the data produced using SK-N-SH cells.

(i) Classification based on two groups comprising treatment with vehicle-control and treatment with any pyrethroid. In this analysis the different pyrethroids were considered as a single group compared with the vehicle-control. Linear forward stepwise discriminant function analysis was applied over 8 steps which resulted in up to 81% classification (Figure 21A). The first ion selected by the modelling was able to classify only 64% of the data and when applied produced a ROC-AUC of just 70%. A combination of data from 3 protein ions produced a model that correctly classified 77% of the data (Figure 21A and B). A multiple regression equation based on these ions using the regression coefficients determined by discriminant function analysis was used to produce a regression equation to describe the relationship and the values calculated for each treatment group shown indicate no clear discrimination between the treatment groups (Figure 21C) although overall there appeared to be some evidence of separation between the control-treated and pyrethroid-treated samples (Figure 21D), with a ROC-AUC of 88%. Thus, it is reasonable to deduce from this that all of the pyrethroids had an effect on the SK-N-SH cells that resulted in a common alteration of their protein profiles, although the effect was not strong.

(ii) Classification based on the effect of type I and type II pyrethroids. The pyrethroids were grouped as type I (allethrin, cis-permethrin, resmethrin and tetramethrin) and type II (α-cypermethrin, β-cyfluthrin, deltamethrin, fenvalerate, fenpropathrin, λ-cyhalothrin) and stepwise linear discriminant function analysis applied to the data. It was found that a single protein ion with m/z = 6674 was able to correctly classify only 65% of the data (Figure 22A) and inclusion of data from other ions only slightly improved the classification. Linear and multiple regression were used to analyse data from m/z = 6674 alone and in combination with up to 3 additional ions. But, in any case it proved difficult to distinguish between the compounds based on classification as type I and type II pyrethroids (Figure 22C-H).

(iii) A novel classification model based on the results obtained using SHS5Y cells. Presentation of the data in the form of a series of volcano plots indicated that none the treatments had a profound effect on the protein profiles (Figure 23), which is consistent with PCA and univariate analyses. Also, the distribution of data was largely symmetrical indicating no clear grouping based on the skewness of the data (Figure 24). Nevertheless, classification based on groups A and B (deduced from the use of SH-SY5Y cells) was attempted, but the data from the SK-N-SH cells failed to support a classification model based on these groups (Figure 25).

Figure 21. Classification of the effect of 10 pyrethroids as a single group compared with vehicle control. Using a forward stepwise approach a discriminant function analysis model was built by inclusion of informative data from a series of ions as indicated in (A). The resultant effect on classification at each step is illustrated in (B). A combination of 3 protein with ions m/z = 8507, 8903, and 9455 produced a model that correctly classified 77% of the data. Regression coefficients calculated from discriminant function analysis of this combination were used to produce a multiple regression equation which describes the relationship. (C) Calculated values for different sample groups. (D) Comparative values in the two groups with the dotted line indicating a cut-off value that correctly classifies 77% of samples. (E) The performance of this classification summarised as a ROC; an AUC of 88% was achieved.

A

Steps	%	m/z
1	64	8903
2	69	9455
3	77	8507
4	75	6605
5	81	6674
6	82	9098

B

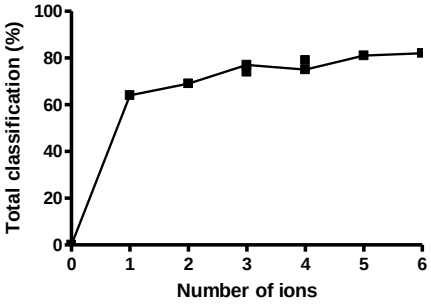

C

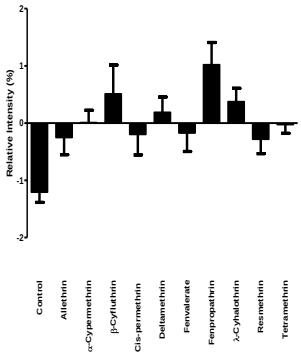

D

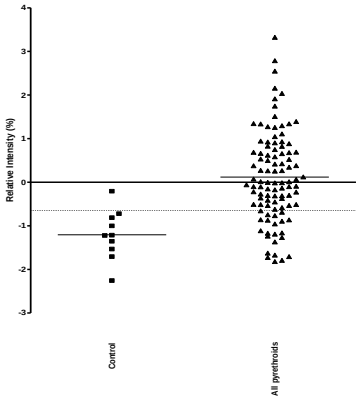

E

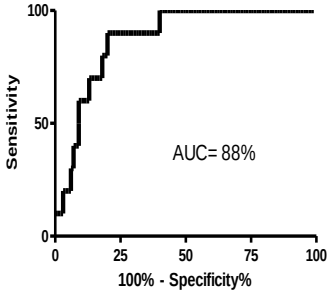

Figure 22. Classification of the effect of type I and type II pyrethroids on protein profiles.
Classification based on assignment as a type I or type II pyrethroid was assessed using forward stepwise discriminant function analysis. (A) Data using the intensity of the m/z = 6674 produced a model that correctly classified 65% of the data. (B) This was improved slightly by inclusion of data from up to 5 ions. (C) Linear regression analysis using the intensity of the m/z 6674 ion failed to distinguish the effect of groups of type I and type II compounds (D) nor individual samples (broken line indicates optimal cut-off). (E) ROC-AUC was 70%. Similarly, multiple regression analysis using 4 ions was insufficient to separate the effects if the type I and type II compounds (F-H).

A

Number	%	m/z
1	65	6674
2	74	10034
3	79	13716
4	81	20819
5	85	6605
6	84	7084

B

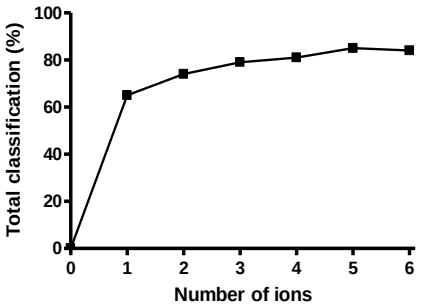

C

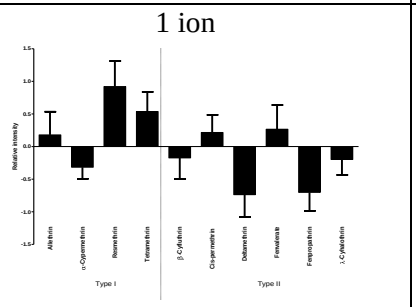

D

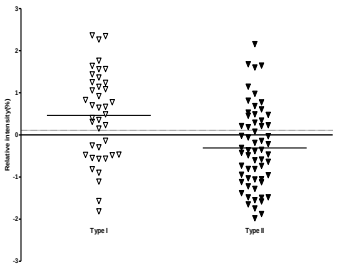

E

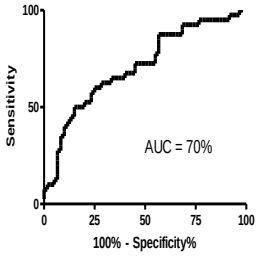

F

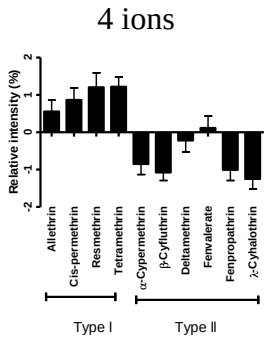

G

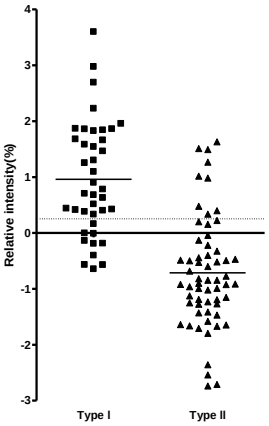

H

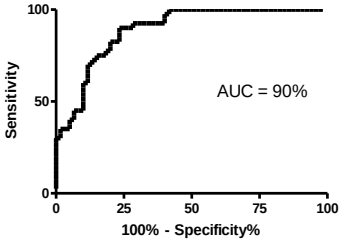

Figure 23. Volcano plots showing the effect of treatment of SK-N-SH cells with 10 pyrethroid compounds. For each protein ion detected the average intensity following treatment with each pyrethroid is expressed as a ratio of the intensity in vehicle-control treated samples and represented as fold change (abscissa) and statistical significance (ordinate). Dotted lines indicate fold changes of 0.8 and 1.2 and a significant level 0.05 (Student's t-test). Overall the majority of the data where within these fold changes and significance levels.

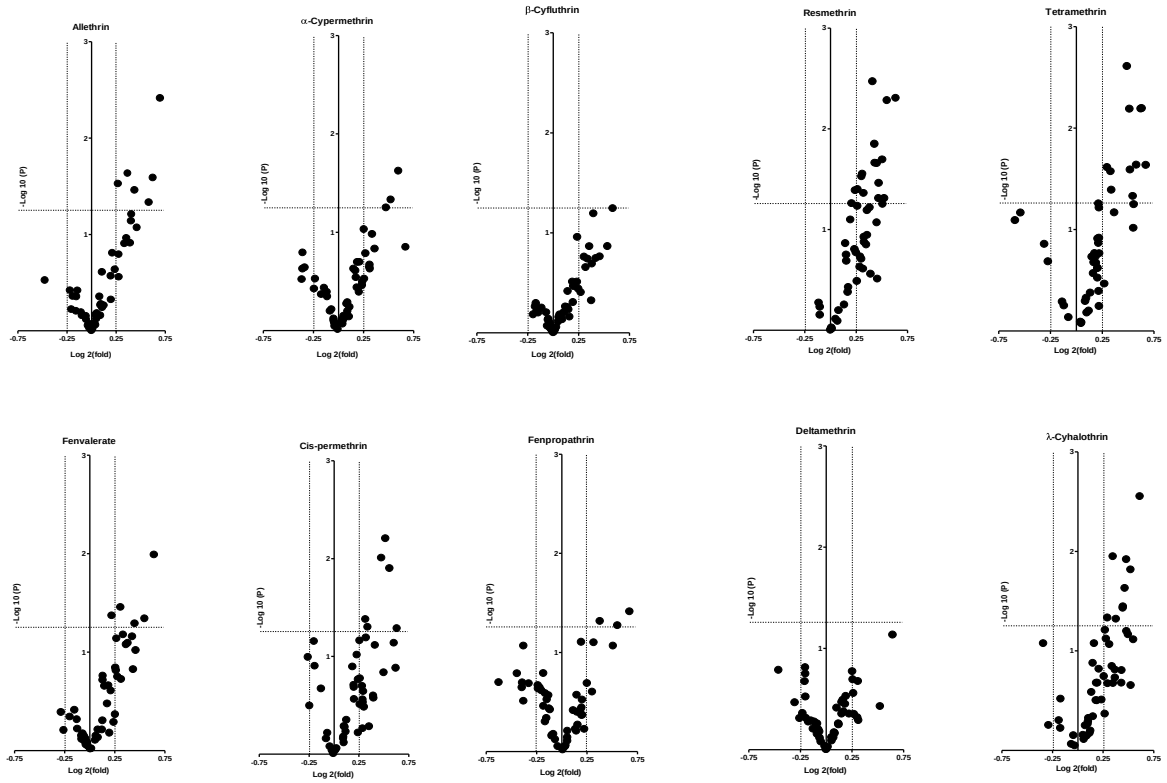

Figure 24. The mean of the $\log_2$(fold) calculation for the volcano plots for SK-N-SH cells treated with 10 pyrethroid compounds. Tukey's multiple comparison test was applied and this showed that there were no statistically significantly differences between any of the treatment groups (p>0.05 in all cases).

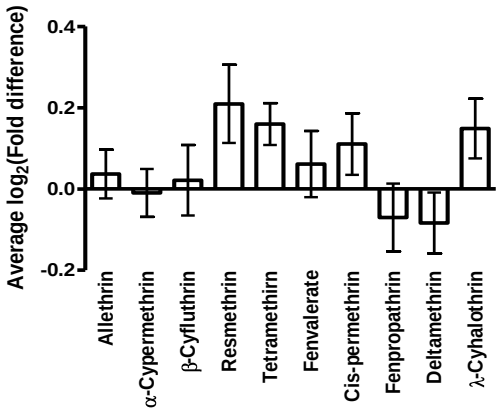

Figure 25. Classification based on the effect of group A and group B pyrethroids on protein profiles of SK-N-SH cells. Classification based on assignment as group A or group B pyrethroids was assessed using forward stepwise discriminant function analysis. (A) A maximum classification of 75% was achieved using two ions of m/z = 27713 and 8903. (B) No improvement on the classification was achieved using data from other ions. (C). Multiple regression modelling based on data from these two ions failed to separate the effect of the different pyrethroids or (D) when presented as groups A and B. (E) The resultant ROC-AUC was 69%.

A

Steps	%	m/z
1	64	27713
2	75	8903
3	62	8507
4	69	12723
5	75	20819

B

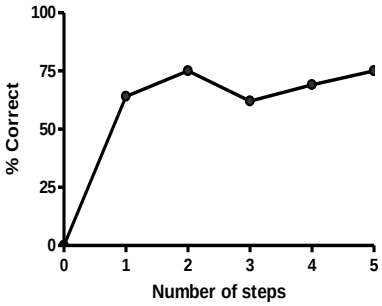

C

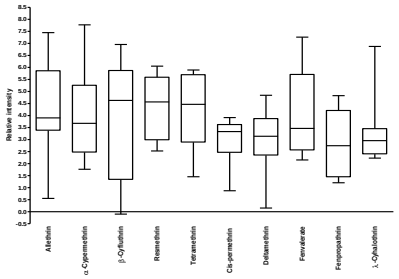

D

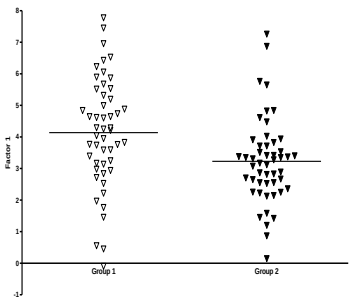

E

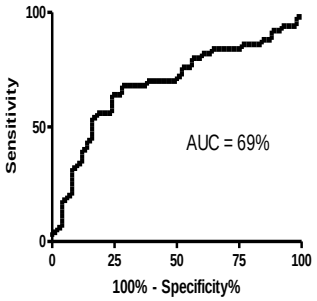

Effect of pyrethroids on HFF-1 cells

Univariate analysis

The relative intensity of 56 ions detected in the SELDI TOF MS spectra were analysed for variation in response to treatment with each of the pyrethroids tested. When analysed individually no statistically significant differences were evident between the control and any of the treatment groups ($p > 0.05$, Student's t-test).

Unsupervised data analysis

The data was subjected to PCA. No grouping was evident from a score plot of the first two principal components (Figure 26), thus this analysis did not give any indication of a common effect of any of the treatment groups.

Supervised Multivariate Analysis

Analyses using PCA and univariate approaches failed to indicate any obvious grouping of the treatment groups. Nevertheless supervised analysis was attempted in the same way as was applied to data from the other cell lines.

(i) Classification based on two groups comprising treatment with vehicle-control and treatment with any pyrethroid. The different pyrethroids were considered as a single group compared with the vehicle-control and linear forward stepwise discriminant function analysis was applied to the data. When applied over 8 steps a classification of 98% was reached. Even so, the relative intensity of a single ion of m/z = 15775 was sufficient to classify 95% of the data into either pyrethroid-treated or vehicle control treated groups (Figure 27). Thus, it appears that all of the pyrethroids had an effect on the HFF-1 cells that resulted in a common alteration that affected the level of the protein represented by the m/z 15775 ion.

(ii) Classification based on type I and type II pyrethroids. The pyrethroids were grouped as type I and type II and stepwise linear discriminant function analysis was applied to the data. It was found that a single protein ion was able to correctly classify only 72% of the data and inclusion of data from other ions only improved the classification slightly (Figure 28A,B). Linear and multiple regression were used to analyse data from m/z = 8513 alone and in combination with m/z=10243, respectively. But, in either case it proved difficult to distinguish between the compounds based on classification as type I and type II pyrethroids (Figure 28C-H).

(iii) A novel classification model based on the results obtained using SH-SY5Y cells. Volcano plots of data obtain following treatment of HFF-1 cells with the different pyrethroids indicated that there was little variation in the levels of the majority of ions (Figure 29). There was no evidence of skewness of the data and no indication of any difference between the effects of the compounds on the distributions (Figure 30). Nevertheless, classification of the data based on the A and B groups identified in the SH-SY5Y cells was attempted. It was found that data from two ions with m/z 13717 and 17788 achieved a classification of just 70% and addition of data from other ions did not improve the classification by very much (Figure 31). This indicated that classification on this basis was not possible, mostly likely due to the lack of effect of the compounds on the protein profiles.

Figure 26. PCA score plot of SELDI TOF MS data produced following treatment of HFF-1 cells with pyrethroids. The score plot shows the first two principal components, PC1 and PC2, and is based on the intensities of all 56 ions detected in SELDI TOF MS protein profiles of the vehicle-control and pyrethroid-treated HFF-1 cells. A histogram showing the 10 variables that contributed most to factors 1 and 2 is shown below.

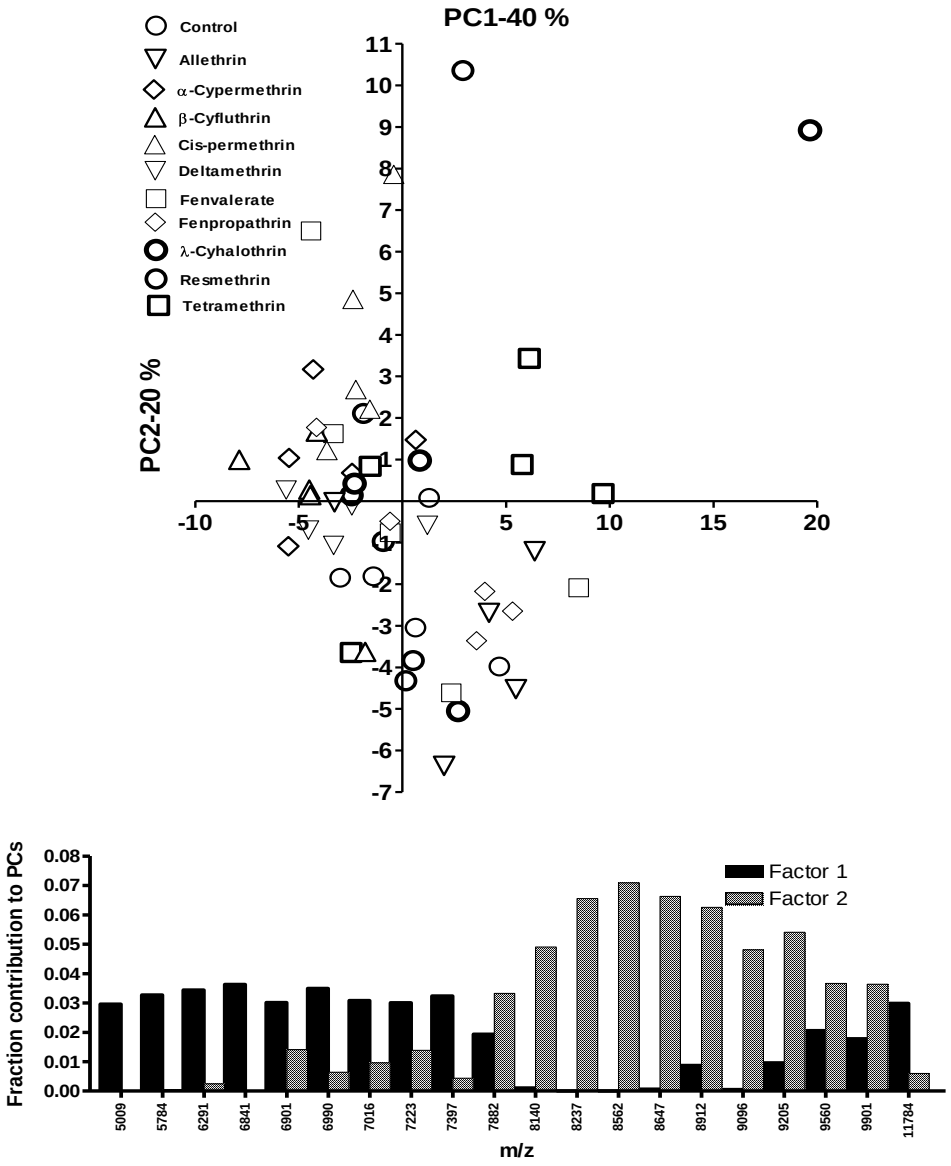

Figure 27. Classification based on the effect of 10 pyrethroids considered as a single group compared with vehicle control. Classification based on assignment as pyrethroid-treated or control-treated was assessed using forward stepwise discriminant function analysis. (A,B) A maximum classification of 98% was achieved using eight ions, although a single ion with m/z 15775 was able to correctly classify 95% of the data (A, B). (C). A simple linear regression model was sufficient to separate the effect of all of the treatment groups from the control group, although there was some overlap (D). (E) The resultant ROC-AUC was 98%.

A

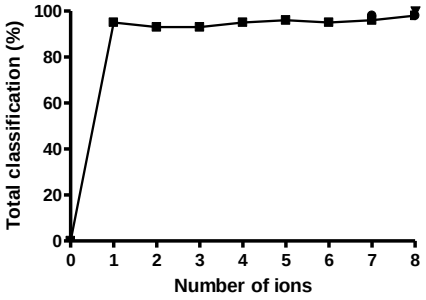

B

Steps	%	m/z
1	95	15775
2	93	17153
3	93	5536
4	95	10243
5	96	10782
6	95	9205
7	96	14566
8	98	8562

C

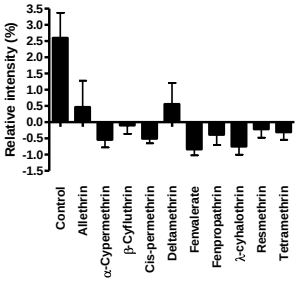

D

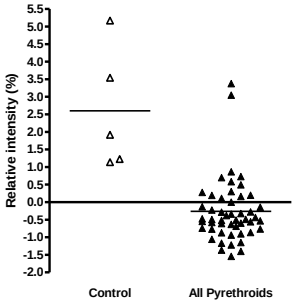

E

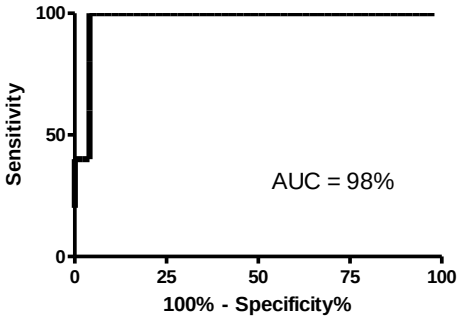

Figure 28. Classification based on the effect of type I and type II pyrethroids. Classification based on assignment as type I or type II pyrethroids was assessed using forward stepwise discriminant function analysis. (A,B) A single ion of m/z = 8513 produced a model that was able to correctly classify 72% of the data; including data from other ions only improved the classification slightly, indeed, including ions in steps 3 and 4 was only possible using a manual approach. (C) A simple linear regression model using the m/z =8513 ion did not successfully differentiate between the effect of the individual compounds (D) nor between the type I and type II compounds. (E) The resultant ROC-AUC was 72%. (F-H) Similarly, multiple regression analysis based on the m/z 8513 and 10243 was unsuccessful in distinguishing between type I and type II pyrethroids.

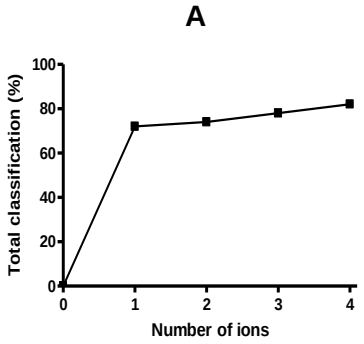

B

Steps	%	m/z
1	72	8513
2	74	10243
3*	78	9901
4*	82	11243

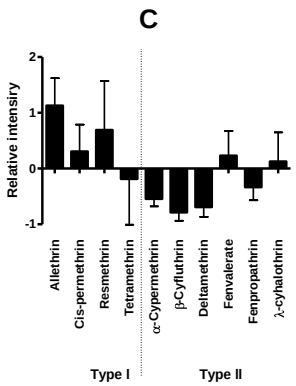

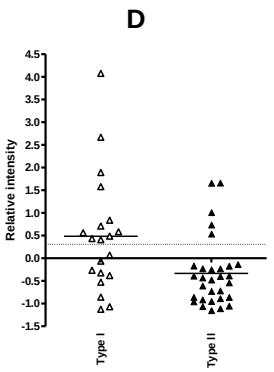

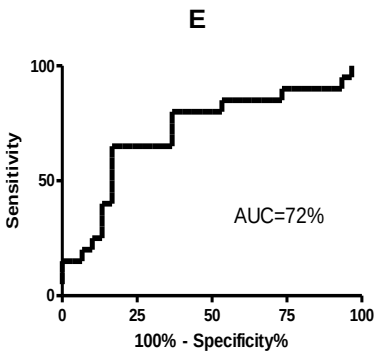

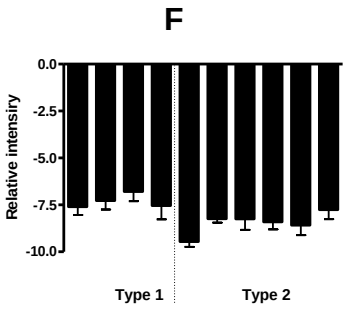

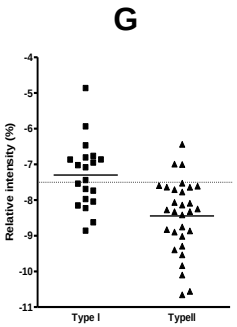

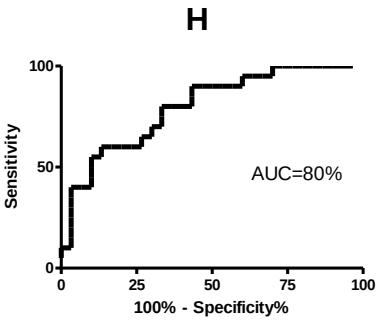

Figure 29. Volcano plots showing the effect of treatment of HFF-1 cells with 10 pyrethroid compounds. For each protein ion detected the average intensity following treatment with each pyrethroid is expressed as a ratio of the intensity in vehicle-control treated samples and represented as fold change (abscissa) and statistical significance (ordinate). Dotted lines indicate fold changes of 0.8 and 1.2 and a significant level 0.05 (Student's t-test). Overall the majority of the data where within these fold changes and significance levels.

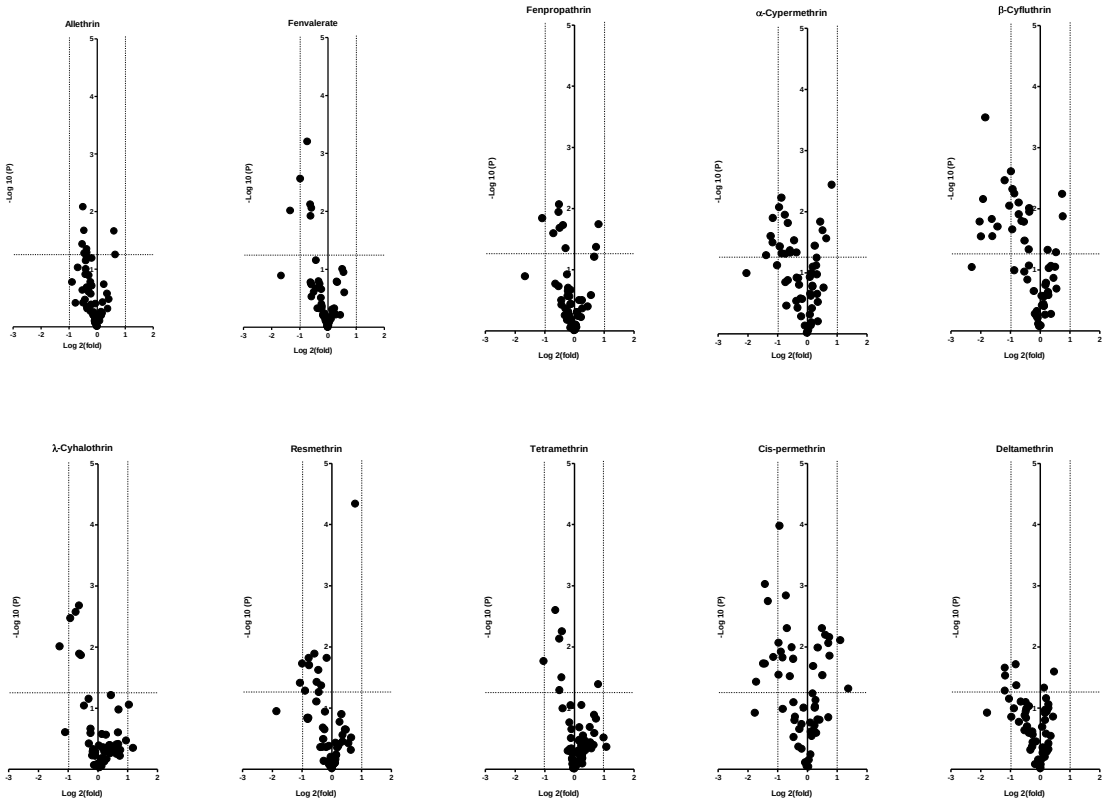

Figure 30. The mean of the $\log_2$(fold) calculation for the volcano plots for HFF-1 cells treated with 10 pyrethroid compounds. Tukey's multiple comparison test was applied and this showed that there were no statistically significantly differences between any of the treatment groups (p>0.05 in all cases).

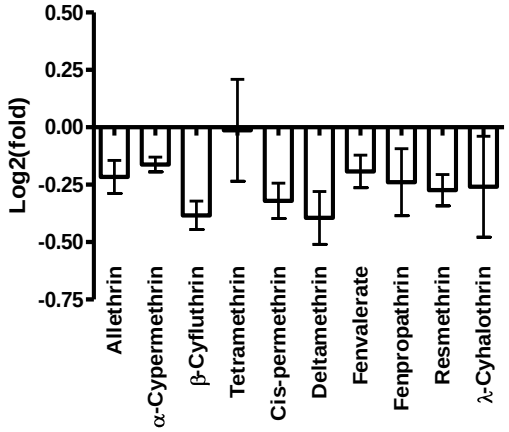

Figure 31. Classification based on the effect of group A and group B pyrethroids. Classification based on assignment as group A or group B pyrethroids was assessed using forward stepwise discriminant function analysis. (A, B) Two ions with m/z = 13717 and 17788 gave a classification of 70%; including data from other ions only improved the classification slightly. (C) A multiple regression equation based on the regression coefficients calculated from discriminant function analysis was applied to the data and was found to discriminate between allethrin and cis-permethrin but not between the other compounds but overall (D) not between the group A and group B compounds. The resultant ROC-AUC was 75%.

.

A

Steps	%	m/z
1	70	13717
2	70	17788
3	74	13933
4	82	7620
5	78	5228

B

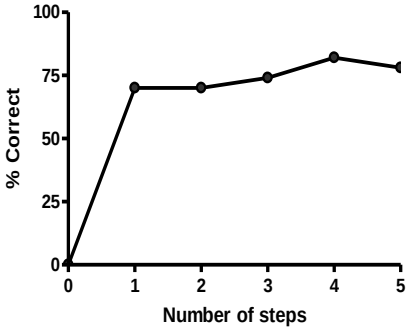

C

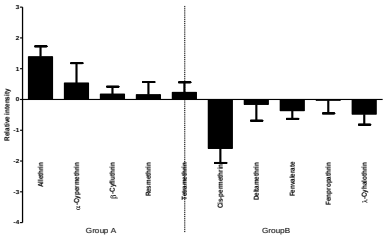

D

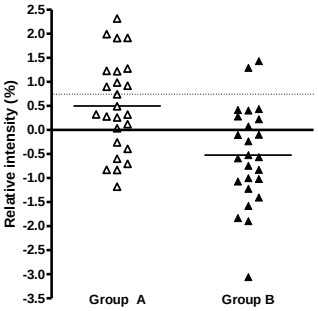

E

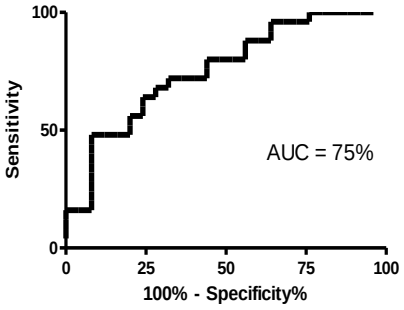

Objective 03: Identification of pathways affected using proteomics

Structural identification of the affected proteins by proteomics will reveal which biochemical pathways are responsive to the various test compounds. This will indicate which pathways are affected by different pyrethrins/pyrethroids.

LC/MS Data Analysis*:* Although SELDI TOF MS was successful in demonstrating the effect of the pyrethroids on SH-SY5Y cells, the only proteins that were identified were histones H2A, H2B, H3 and H4. In order to obtain a more comprehensive profile of responsive proteins an LC/MS-based analysis was also performed. As this was quite time consuming the experiment was limited to the analysis of the effect of four compounds, which were deltamethrin, λ-cyhalothrin, resmethrin and tetramethrin. The effect of both deltamethrin and λ-cyhalothrin was evident in SELDI-TOF MS analysis and were classified into group B (and are also type II pyrethroids) whereas resmethrin and tetramethrin were placed in group A (and are also type I pyrethroids). SH-SY5Y cells were treated with each of the four pyrethroids and vehicle alone as described in the Methods section using the same concentrations that were used in the SELDI-TOF MS experiments. The cells were lysed, protein content measured and separated by SDS-PAGE (Figure 32). The proteins were excised, digested with trypsin and the resultant peptides analysed by LC-MS as described in the Methods section.

Figure 32. SDS-PAGE separation of SH-SY5Y proteins in preparation for LC-MS analysis. Flasks of SH-SY5Y cells (n=5) were treated with each pyrethroid and whole cell preparations were subjected to SDS PAGE using 10% gels. The example shows a gel of SH-SY5Y cell homogenates following treatment with vehicle control (C1-5), deltamethrin (D1-5) and λ-cyhalothrin (L1-5) and then stained with Instant Blue. Each lane was cut into 20 slices as indicted. The gel pieces were then de-stained, the proteins they contain digested with trypsin and the resultant peptides extracted in preparation for LC-MS.

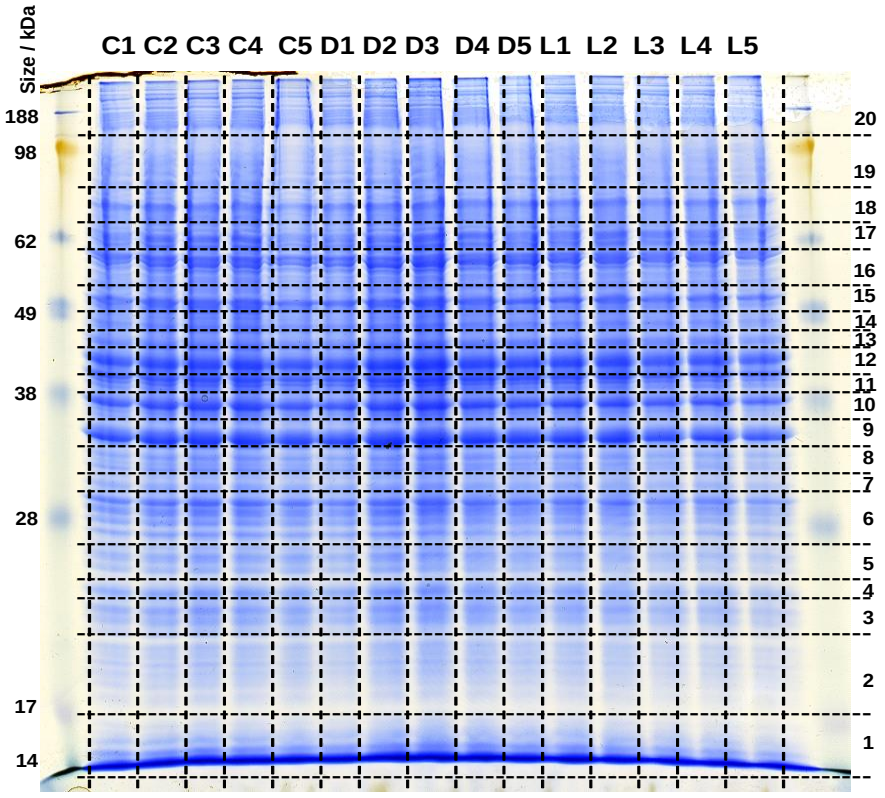

A total of 985 proteins were identified based on identification of at least 2 unique peptides for each protein. Statistical differences between the mean normalised abundances of these proteins in the five

treatment groups were determined by ANOVA and indicated statistical differences ($p<0.05$) in the levels of 306 proteins. *Post hoc* analysis was performed by comparing calculated protein abundances in each of the pyrethroid treatment groups with those in the vehicle-control group. By comparing the effects of the compounds on the up or down regulation of individual proteins it was possible to establish several patterns of response to summarise the data. Four main patterns were recognised (Table 5). For each protein, where possible the profile of response to the pyrethroids that best fitted one of these four patterns was selected. The criteria for matching was (a) complete identity with statistically significant changes that matched one of the patterns of up or down regulation, (b) 3 out of 4 statistically significant changes that matched the pattern of up or down regulation (with the other value indicating up or down regulation consistent with the pattern, even though it did not reach statistical significance), (c) 2 out of 4 statistically significant changes that matched the pattern of up or down regulation (with the other values indicating up or down regulation consistent with the pattern, even though they did not reach statistical significance), (d) 2 out of 4 statistically significant changes that either matched to more than one of the patterns of up or down regulation, or could not be matched to any of the patterns were collected together as group (v), or (e) where only one of the compounds caused a statistically significant change data was not considered further. In all, 153 proteins were represented in one of the five classification groups. The proteins identified in each of the groups are listed in Table 6.

Table 5. Patterns of differences in protein expression following treatment of SH-SY5Y cells with four different pyrethroids. In group (i) proteins with both deltamethrin and λ-cyhalothrin were up regulated and with resmethrin and tetramethrin were down regulated compared to the control. In group (ii) proteins with both deltamethrin and λ-cyhalothrin were down regulated and with resmethrin and tetramethrin were up regulated compared to the control. In group (iii) proteins with deltamethrin, λ-cyhalothrin, resmethrin and tetramethrin were up regulated compared to the control. In group (iv) proteins with deltamethrin, λ-cyhalothrin, resmethrin and tetramethrin were down regulated compared to the control. Group (v) comprising those proteins whose patterns of expression are not represented in groups (i)-(iv).

Group	Deltamethrin	λ-Cyhalothrin	Resmethrin	Tetramethrin	No of proteins
(i)	↑	↑	↓	↓	61
(ii)	↓	↓	↑	↑	26
(iii)	↑	↑	↑	↑	18
(iv)	↓	↓	↓	↓	34
(v)	Other patterns				14

↑= up regulated, ↓= down regulated.

Notably, there was a similar response of the cells to treatment with deltamethrin and λ-cyhalothrin and of those treated with resmethrin and tetramethrin. The response is similar to that found for these compounds using SELDI TOF MS analysis with deltamethrin and λ-cyhalothrin being grouped together in group B and resmethrin and tetramethrin into group A (Table 3).

In order to better understand the function of all of the proteins that responded to treatment the list of identified proteins that responded to treatment in each of the response groups (i)-(v) were analysed using PANTHER which classified them based on various biological processes. The results shown in Figure 33 indicate that the majority of proteins in all of the groups are involved in metabolism, transport and cell structure and motility. As most were in the metabolism group, this group was subdivided and showed that the majority were involved in nucleoside and nucleic acid metabolism, especially in groups (i) and (ii).

Figure 33. Categorisation of pyrethroid responsive proteins. The proteins were classified into different biological processes as indicted in (A). Overall the majority of proteins were in the metabolism group and so these proteins were further classified as shown in (B).

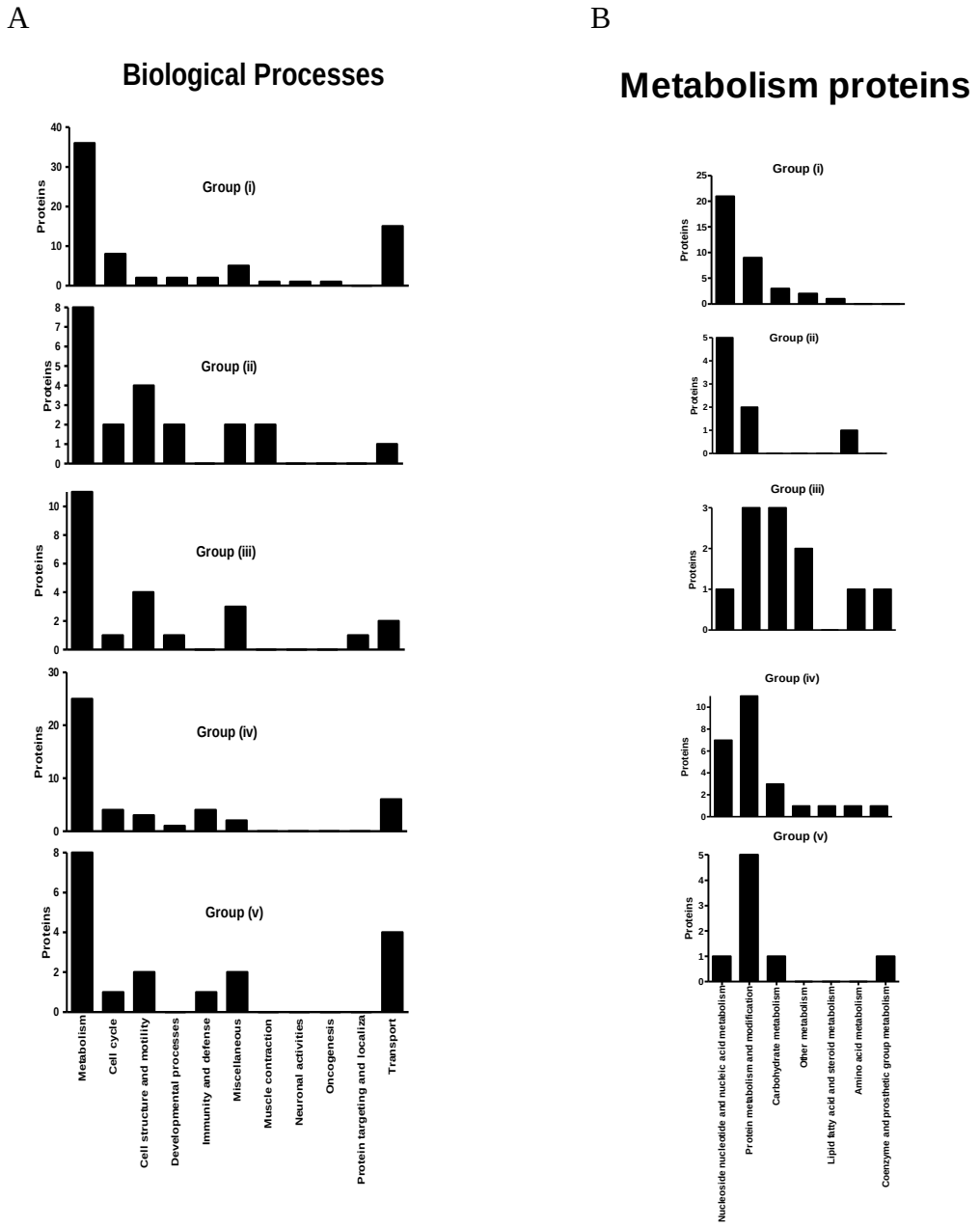

Several of the nucleoside and nucleic acid metabolism proteins have roles in DNA repair and protein synthesis, and some of their functions are summarised in Table 7. The DNA repair proteins are part of the neuronal cellular defence DNA damage response system (Barzilai et al., 2008). One activator of the DNA damage response is double stranded breaks in DNA. Both RAD50 and prohibitin (a p53 binding protein) are involved and were found here. They are recruited to sites of double strand breaks in DNA and are an early response to damage (Barzilai et al., 2008). The double strand break response is involved in a series of intracellular pathways leading to DNA repair and maintenance of the integrity of genomic DNA. Part of this cascade involves proteins associated with chromatin organisation and the activation of cell cycle check points that temporarily arrest the cell cycle until the damage has been assessed and repaired. The Structural Maintenance Of Chromosomes 3 protein and the DNA Mismatch Repair Msh6 protein may have a role here. The Structural Maintenance Of Chromosomes 3 protein is involved in chromatin cohesion (which is part of chromatin reorganisation) and the DNA Mismatch Repair protein Msh6 is a

DNA checkpoint protein (Francisconi et al., 2005). Perhaps related to this is an increase in the Cold-Inducible mRNA Binding Protein, which has been shown to be activated following DNA damage and upon mild cold shock and others conditions of stress. The molecular mechanisms by which cells respond to cold stress involve a series of events that modulate gene transcription, translation, the cell cycle and metabolic processes (Lleonart, 2010) and this would be consistent with increases in several proteins involved in nucleotide and nucleoside metabolism, RNA splicing, protein stability and protein synthesis (see Table 7).

In part the pattern of changes exhibited in group (i) resembles a cellular response to a mutagenic compound, especially with respect to increases in DNA repair proteins. However, Ames testing indicates that deltamethrin, resmethrin and λ-cyhalothrin lack any mutagenic activity and although tetramethrin was reported to give weakly positive results this may have been due to an unidentified contaminant. In the experiments performed in this current work the quantities of these compounds used were less than those that caused overt cytotoxicity and so it appears that increases in DNA repair proteins represent the consequence of exposure to subacute concentrations of the pyrethroids. Certainly, at the doses used, DNA was not damaged to the extent that repair mechanisms were ineffective and the cells were committed to apoptosis as cell viability was maintained. Also, interestingly, the pattern of protein alterations of the cells to deltamethrin and λ-cyhalothrin were similar but contradictory to that produced by resmethrin and tetramethrin. Presumably this indicates some fundamental difference in the response of the cells through these compounds. Future experiments aimed to identify the primary causes of these responses will be informative for understanding the toxicity of these compounds.

Objective 04: Confirmation of functional role of identified proteins

Once proteins involved in pathways affected by the pyrethrins/pyrethroids have been identified, their contribution to the functional changes induced by the compounds will be determined using small interference RNA species, targeted to each protein in turn.

Unfortunately, there was insufficient time to pursue this objective.

Table 6. Proteins identified in SH-SY5Y cells that responded to treatment with the pyrethroids deltamethrin (D), λ-cyhalothrin (L), resmethrin (R), and tetramethrin (T). The numbers of tryptic peptides that were used in the identification of each protein and in the assessment of relative levels are shown. Slice indicates the position in the gel the proteins occurred. The relative fold change resulting from each pyrethroid compared with the control (C) is indicated along with the statistical significance of the difference between the control (Student's t-test).

Description	NCBI accession number	Number of Peptides	Slice	Probability				Fold change			
				D	L	R	T	D/C	L/C	R/C	T/C
Group (i)											
Actin-related protein 2 isoform b	NP_005713.1	4	8	**<0.01**	**0.03**	0.47	**0.01**	1.90	1.60	0.82	0.24
Acyl-CoA thioesterase 7 isoform hBACHbapi	NP_863654.1	7	8	**<0.01**	0.25	0.28	**0.03**	1.31	1.13	1.12	0.68
Adenylosuccinate synthase	NP_001117.2	4	10	**0.01**	**<0.01**	0.18	**0.02**	1.33	1.49	1.14	0.75
Autoantigen RCD8	NP_055144.3	4	19	0.06	**0.02**	**0.03**	**0.02**	1.23	1.31	0.78	0.68
BUB3 budding uninhibited by benzimidazoles 3 isoform	NP_004716.1	5	8	**0.01**	**0.01**	0.12	0.10	1.35	1.31	0.74	0.69
Calponin 3	NP_001830.1	5	8	**<0.01**	0.42	0.16	**<0.01**	1.67	1.18	0.68	0.31
Chaperonin containing TCP1, subunit 4 (delta)	NP_006421.2	20	12	0.31	0.34	**0.01**	**<0.01**	1.08	1.10	0.79	0.71
Chromatin-specific transcription elongation factor	NP_009123.1	11	19	**0.03**	**0.02**	**0.02**	**0.01**	1.64	1.68	0.28	0.27
Clathrin heavy chain 1	NP_004850.1	56	19	**0.03**	**0.02**	0.06	0.19	1.28	1.29	0.76	0.79
Cold inducible RNA binding protein	NP_001271.1	3	1	**0.03**	0.41	**0.04**	**0.05**	1.35	1.16	0.64	0.57
COP9 signalosome subunit 5	NP_006828.2	5	7	**<0.01**	**<0.01**	**0.03**	0.22	2.31	2.77	0.70	0.75
DEAD (Asp-Glu-Ala-Asp) box polypeptide 46	NP_055644.2	4	19	**0.04**	0.06	**0.01**	**0.01**	1.58	1.51	0.18	0.13
DEAH (Asp-Glu-Ala-His) box polypeptide 9	NP_001348.2	26	19	**0.03**	**0.02**	**0.02**	**0.02**	1.59	1.65	0.32	0.34
Dynactin 1 isoform 1	NP_004073.2	11	19	**0.04**	**0.03**	**0.02**	**0.03**	1.32	1.32	0.64	0.64
Enolase 2	NP_001966.1	9	10	**0.01**	0.38	**<0.01**	0.05	1.13	1.05	0.82	0.76
Eukaryotic translation elongation factor 1 alpha	NP_001393.1	8	11	**<0.01**	0.09	0.22	**0.02**	2.15	0.75	1.25	0.65
Family with sequence similarity 98, member B	NP_775882.2	5	10	**0.04**	0.32	0.16	**0.05**	1.21	1.09	0.82	0.81
G protein pathway suppressor 1 isoform 1	NP_997657.1	3	12	**0.01**	0.69	0.16	**0.02**	1.42	0.92	0.83	0.64
General transcription factor II, i isoform 3	NP_127494.1	9	19	**0.03**	0.11	**0.02**	**0.02**	1.60	1.42	0.34	0.36
Glutamyl-prolyl tRNA synthetaseapiens	NP_004437.2	19	19	**0.04**	**0.02**	0.32	0.10	1.22	1.26	0.89	0.80
Glutathione reductase	NP_000628.2	5	11	**0.02**	0.83	0.33	**0.03**	1.27	0.98	1.11	0.74
GNAS complex locus isoform aapiens	NP_000507.1	4	10	**0.01**	0.28	0.09	**0.03**	1.26	1.10	0.84	0.77
Guanine nucleotide binding protein (G protein),	NP_002058.2	3	8	**0.01**	**0.01**	0.32	0.08	1.54	1.65	0.80	0.48
Heterogeneous nuclear ribonucleoprotein C	NP_001070910.1	8	8	**0.01**	0.10	0.29	**0.02**	1.19	1.22	1.10	0.77
Heterogeneous nuclear ribonucleoprotein D	NP_001003810.1	6	10	**<0.01**	0.37	0.20	**0.04**	1.41	1.09	0.87	0.76
Heterogeneous nuclear ribonucleoprotein F	NP_001091678.1	8	10	**0.04**	0.54	**<0.01**	0.08	1.06	0.97	0.87	0.81

Description	NCBI accession number	Number of Peptides	Slice	Probability				Fold change			
				D	L	R	T	D/C	L/C	R/C	T/C
IQ motif containing GTPase activating protein 1	NP_003861.1	5	19	**0.02**	0.06	**0.04**	0.08	1.56	1.43	0.54	0.61
Isoleucyl-tRNA synthetase	NP_038203.2	9	19	**0.04**	0.07	**0.04**	0.09	1.34	1.30	0.64	0.69
Leucine-rich PPR motif-containing protein	NP_573566.2	31	19	**0.01**	**0.01**	**0.02**	**0.03**	1.87	1.87	0.27	0.36
Matrin 3	NP_061322.2	3	19	0.07	0.88	**0.02**	**0.05**	1.78	1.05	0.13	0.27
DNA mismatch repair protein Msh6	NP_000170.1	11	19	**0.05**	**0.03**	0.05	0.13	1.31	1.36	0.69	0.73
Myosin IB	NP_036355.2	3	19	0.09	0.07	**0.02**	**0.03**	1.47	1.51	0.33	0.40
Nuclear autoantigenic sperm protein isoform 2	NP_002473.2	6	19	**0.01**	**0.01**	0.09	**0.01**	1.37	1.38	0.72	0.57
Nucleolar and coiled-body phosphoprotein 1	NP_004732.2	3	19	**0.01**	0.10	**0.03**	**0.02**	2.03	1.64	0.17	0.08
Nucleoporin 155kDa isoform 1	NP_705618.1	4	19	**0.04**	**0.03**	**0.01**	**0.02**	1.55	1.61	0.26	0.32
Nucleoporin 160kDa	NP_056046.1	3	19	0.10	**0.02**	**0.02**	**0.01**	1.18	1.30	0.68	0.67
Oxygen regulated protein precursor	NP_006380.1	26	19	**0.01**	**0.01**	0.16	0.11	1.45	1.44	0.79	0.76
P30 DBC protein	NP_954675.1	9	19	**0.02**	0.47	**0.01**	**0.01**	1.75	1.21	0.19	0.24
Phosphoribosylformylglycinamidine synthase	NP_036525.1	8	19	**0.03**	**0.02**	**0.02**	0.11	1.48	1.52	0.44	0.56
Poly(rC)-binding protein 2 isoform bapien	NP_114366.1	4	8	**0.01**	0.42	0.35	**0.04**	1.71	1.20	0.81	0.45
PREDICTED: similar to 40S ribosomal protein	xp_944831.1	4	9	**0.01**	0.31	0.72	**0.01**	1.52	1.23	0.93	0.56
PREDICTED: similar to Proteasome	xp_001131778.1	3	19	0.49	**<0.01**	**0.02**	0.65	1.12	1.36	0.76	0.92
PREDICTED: similar to sorbitol dehydrogenase	xp_001132175.1	6	8	**<0.01**	0.13	**0.02**	**0.01**	1.91	1.66	0.32	0.23
Prohibitin	NP_002625.1	8	4	0.37	**0.01**	**0.01**	**0.01**	1.07	1.25	0.81	0.81
Proline, glutamic acid and leucine rich protein	NP_055204.2	7	19	**0.01**	**<0.01**	**0.05**	0.24	1.42	1.47	0.71	0.81
Protein disulfide isomerase-associated 4ap	NP_004902.1	11	16	**0.02**	0.13	0.62	**<0.01**	1.15	0.84	0.95	0.61
protein kinase C substrate 80K-H isoform 1	NP_002734.2	6	17	**<0.01**	0.78	0.97	**0.02**	1.37	1.03	1.00	0.71
DNA repair protein RAD50	NP_597816.1	5	19	**<0.01**	**0.01**	**0.05**	0.92	1.52	1.43	0.71	0.98
ribosomal protein L3 isoform aapiens	NP_000958.1	9	10	**<0.01**	**0.01**	0.65	0.46	1.55	1.41	0.94	0.88
Splicing factor 3b, subunit 3	NP_036558.3	14	19	**0.02**	**0.03**	**0.03**	**0.04**	1.61	1.57	0.41	0.48
Squamous cell carcinoma antigen recognized by T cells	NP_055521.1	4	19	**0.05**	**0.05**	**0.01**	**0.02**	1.57	1.57	0.26	0.31
Staphylococcal nuclease domain containing 1	NP_055205.2	3	17	0.68	**<0.01**	**0.03**	0.80	0.85	2.28	0.15	0.90
Structural maintenance of chromosomes 3	NP_005436.1	6	19	**0.04**	**0.03**	**0.03**	**0.01**	1.44	1.47	0.52	0.42
SUMO1 activating enzyme subunit 1	NP_005491.1	5	8	0.13	**0.02**	0.35	**<0.01**	1.16	1.25	0.91	0.63
SWI/SNF-related matrix-associated actin-dependent	NP_003066.2	7	19	**0.03**	**0.01**	0.09	0.12	1.40	1.48	0.70	0.73
Ubiquitin associated protein 2-likeapiens	NP_055662.2	5	19	**0.04**	**0.04**	0.05	**0.04**	1.34	1.33	0.68	0.65
Vacuolar protein sorting 26 A isoform 1ap	NP_004887.2	4	7	0.11	0.26	**0.05**	**<0.01**	1.24	1.26	0.71	0.35

Description	NCBI accession number	Number of Peptides	Slice	Probability				Fold change			
				D	L	R	T	D/C	L/C	R/C	T/C
Valyl-tRNA synthetase	NP_006286.1	6	19	**0.02**	**0.02**	**0.02**	**0.03**	1.67	1.68	0.34	0.40
Vesicle amine transport protein 1	NP_006364.2	5	10	**0.02**	0.58	0.12	**<0.01**	1.13	0.96	0.87	0.75
VGF nerve growth factor inducible precursor	NP_003369.2	5	17	**0.02**	0.89	**0.02**	**<0.01**	1.46	0.97	0.49	0.23
WD repeat domain 57 (U5 snRNP specific)a	NP_004805.2	3	7	0.10	0.11	**0.02**	**0.02**	1.22	1.44	0.66	0.43
Group (ii)											
Chromatin-specific transcription elongation factor	NP_009123.1	7	18	0.70	0.12	**<0.01**	**<0.01**	0.91	0.62	2.55	2.53
DEAH (Asp-Glu-Ala-His) box polypeptide 9	NP_001348.2	11	18	0.05	0.05	**<0.01**	**<0.01**	0.54	0.55	2.36	2.27
DEK oncogene	NP_003463.1	3	10	0.02	0.21	**0.01**	0.05	0.55	0.81	1.65	1.46
Eukaryotic translation initiation factor 5B	NP_056988.3	4	19	0.10	0.11	**0.01**	0.03	0.76	0.78	1.54	1.52
H2A histone family, member V isoform 1	NP_036544.1	3	2	0.03	**<0.01**	0.10	0.81	0.83	0.73	1.17	1.04
Keratin 10	NP_000412.2	4	17	0.01	**0.01**	0.26	**<0.01**	0.37	0.29	1.56	6.93
Keratin 10	NP_000412.2	3	13	0.01	0.02	0.45	**<0.01**	0.18	0.26	1.64	3.62
Keratin 10	NP_006112.3	8	16	0.04	0.78	0.36	**<0.01**	0.61	1.05	1.29	7.58
Keratin 10	NP_000412.2	7	15	0.04	0.48	0.93	**<0.01**	0.37	0.74	0.94	6.50
Keratin 10	NP_000412.2	4	16	0.02	0.07	0.68	**<0.01**	0.51	0.61	1.22	5.25
Keratin 2	NP_000414.2	4	13	**<0.01**	0.04	0.95	**<0.01**	0.23	0.43	1.02	1.92
Keratin 2	NP_000414.2	3	11	**<0.01**	0.55	0.21	**0.01**	0.39	0.86	1.28	6.37
Keratin 9	NP_000217.2	12	17	0.01	0.05	0.71	**0.01**	0.32	0.48	0.88	13.51
Keratin 9	NP_000217.2	7	16	0.04	0.35	0.57	**<0.01**	0.31	0.69	1.26	14.98
Keratin 9	NP_000217.2	7	4	0.01	0.31	0.61	**<0.01**	0.50	1.74	1.47	14.12
Keratin 9	NP_000217.2	10	15	0.01	0.36	0.29	**<0.01**	0.41	0.73	0.75	12.20
Leucine-rich PPR motif-containing protein	NP_573566.2	18	18	0.07	0.09	**<0.01**	**<0.01**	0.61	0.64	1.94	2.30
Nuclear distribution gene C homolog	NP_006591.1	5	9	0.02	0.05	0.05	0.42	0.17	0.34	1.69	1.24
Phosphoserine aminotransferase isoform 1	NP_478059.1	4	8	0.06	0.02	0.03	0.56	0.79	0.73	1.53	1.09
PREDICTED: similar to peptidylprolyl isomerase A	XP_931592.2	6	1	**0.01**	0.04	0.03	0.73	0.18	0.42	1.60	1.10
PREDICTED: similar to peptidylprolyl isomerase A	XP_001130327.1	3	1	0.01	0.11	**<0.01**	0.83	0.44	0.69	1.78	1.05
Profilin 1	NP_005013.1	5	1	0.02	0.02	0.03	0.43	0.20	0.23	1.96	0.74
Reticulocalbin 2, EF-hand calcium binding domain	NP_002893.1	5	11	0.48	**<0.01**	0.04	0.26	0.95	0.76	1.27	1.22
Sorcin isoform a	NP_003121.1	3	2	0.04	0.20	**<0.01**	0.06	0.83	0.91	1.28	1.30
Splicing factor proline/glutamine rich	NP_005057.1	12	17	0.65	0.02	**<0.01**	0.26	0.97	0.83	1.26	1.09

Description	NCBI accession number	Number of Peptides	Slice	Probability				Fold change			
				D	L	R	T	D/C	L/C	R/C	T/C
Transgelin 2	NP_003555.1	7	2	0.10	0.24	**0.01**	0.03	0.93	0.94	1.28	1.12
Group (iii)											
6-phosphogluconolactonase	NP_036220.1	5	4	0.02	0.46	0.01	0.51	1.33	0.93	1.37	1.05
Abhydrolase domain containing 10	NP_060864.1	3	4	0.09	0.89	0.03	**<0.01**	1.28	1.01	1.53	1.41
Acetyl-Coenzyme A acetyltransferase 2	NP_005882.2	6	8	0.03	0.06	0.02	0.11	1.18	1.14	1.36	0.75
Aldehyde dehydrogenase 9A1	NP_000687.3	3	11	0.04	0.05	**<0.01**	0.52	1.15	0.88	1.30	1.05
Beta isoform of regulatory subunit A	NP_859050.1	8	14	0.01	0.20	0.01	0.42	1.32	0.75	1.19	0.90
Fumarate hydratase precursor	NP_000134.2	8	10	**<0.01**	**<0.01**	0.27	0.65	1.32	1.24	1.09	1.04
Karyopherin alpha 6 [	NP_036448.1	3	13	0.02	0.85	**<0.01**	0.19	1.29	1.02	1.37	1.10
Keratin 16	NP_005548.2	4	11	**<0.01**	0.35	0.01	**<0.01**	1.37	0.89	1.50	2.57
Keratin 5	NP_000415.2	5	7	0.06	**<0.01**	0.86	0.02	0.64	1.68	1.09	4.94
LUC7-like 2	NP_057103.2	3	11	**<0.01**	0.34	0.05	0.51	1.61	0.88	1.40	0.88
Mitochondrial short-chain enoyl-coenzyme A hydrat	NP_004083.2	3	4	0.38	0.63	0.01	0.04	1.22	1.09	2.15	1.64
PREDICTED: similar to Phosphoglycerate mutase 1	XP_932047.1	4	4	0.04	0.39	**0.01**	0.05	1.49	0.85	1.96	1.49
Prolyl 4-hydroxylase, beta subunit precursor	NP_000909.2	7	13	0.01	0.16	**<0.01**	**0.01**	1.75	1.19	1.55	1.40
Proteasome beta 3 subunit	NP_002786.2	4	3	0.74	**<0.01**	**<0.01**	**<0.01**	1.06	1.32	1.70	1.46
Rho GTPase activating protein 1	NP_004299.1	5	11	0.01	0.82	**<0.01**	0.50	1.15	0.99	1.22	0.93
Splicing factor 3b, subunit 3	NP_036558.3	6	18	0.60	0.48	**<0.01**	**<0.01**	1.49	1.24	2.08	3.93
Triosephosphate isomerase 1	NP_000356.1	4	4	0.30	0.67	**0.01**	0.04	1.22	1.09	1.94	1.75
Tubulin alpha 6	NP_116093.1	4	13	0.04	0.80	0.02	0.28	1.50	1.05	2.33	1.24
Group (iv)											
Actin-like 6A isoform 1	NP_004292.1	3	10	0.29	0.01	0.78	**<0.01**	1.09	0.84	0.98	0.62
Albumin precursor	NP_000468.1	6	15	0.01	**<0.01**	**<0.01**	**<0.01**	0.47	0.41	0.51	0.43
Ataxin 10	NP_037368.1	3	10	0.85	**<0.01**	0.31	0.02	0.99	0.78	0.95	0.80
Beta actin	NP_001092.1	4	7	0.07	0.19	0.01	**<0.01**	0.80	0.77	0.73	0.50
Cathepsin D preproprotein	NP_001900.1	3	4	**<0.01**	0.34	**<0.01**	0.18	0.61	1.27	0.46	0.82
C-terminal binding protein 2 isoform 1	NP_001320.1	3	10	0.26	0.30	0.02	**0.01**	0.93	0.92	0.83	0.73
Dihydropyrimidinase-like 2	NP_001377.1	6	16	0.17	**<0.01**	0.42	**<0.01**	1.09	0.76	0.92	0.66
Enolase 1	NP_001419.1	18	10	0.89	0.10	**<0.01**	0.01	1.00	0.93	0.87	0.82

Description	NCBI accession number	Number of Peptides	Slice	Probability				Fold change			
				D	L	R	T	D/C	L/C	R/C	T/C
ErbB3-binding protein 1	NP_006182.2	9	10	0.27	0.03	0.07	**<0.01**	1.07	0.87	0.88	0.78
Eukaryotic translation elongation factor 1 alpha	NP_001393.1	20	10	0.02	0.19	0.05	**<0.01**	0.86	0.91	0.90	0.79
Eukaryotic translation initiation factor 6	NP_852133.1	3	3	0.04	**0.01**	0.78	**<0.01**	0.82	0.83	0.98	0.73
Glutathione-S-transferase omega 1	NP_004823.1	3	4	**<0.01**	0.95	**<0.01**	0.52	0.47	1.01	0.50	0.89
Heat shock 70kD protein binding protein	NP_003923.2	3	10	**<0.01**	0.05	0.16	0.03	0.62	0.86	0.91	0.83
Heat shock 70kDa protein 9 precursor	NP_004125.3	7	16	0.11	0.01	0.59	0.01	0.49	0.15	0.81	0.16
Heat shock 90kDa protein 1, beta	NP_031381.2	5	17	0.77	0.07	**<0.01**	**<0.01**	0.96	0.77	0.60	0.49
Heat shock protein 90kDa alpha (cytosolic)	NP_005339.3	4	17	0.42	0.07	0.02	**<0.01**	0.88	0.72	0.65	0.48
Mitochondrial short-chain enoyl-coenzyme A	NP_004083.2	5	3	**0.01**	0.12	0.01	**<0.01**	0.66	0.88	0.70	0.68
Non-POU domain containing, octamer-binding	NP_031389.3	13	12	0.17	0.21	**<0.01**	**<0.01**	0.92	0.89	0.78	0.79
Nuclease sensitive element binding protein 1	NP_004550.2	4	10	0.63	**0.01**	0.13	**<0.01**	1.02	0.86	0.91	0.76
Nucleolin	NP_005372.2	16	17	0.01	**<0.01**	0.58	**<0.01**	0.89	0.84	0.97	0.85
Phosphoribosylglycinamide formyltransferase,	NP_780294.1	5	11	0.13	0.01	0.15	**<0.01**	0.86	0.81	1.14	0.70
PREDICTED: similar to Phosphoglycerate mutase 1	XP_932047.1	3	3	**<0.01**	0.85	**0.01**	**<0.01**	0.48	1.04	0.53	0.46
Prolyl 4-hydroxylase, beta subunit precursor	NP_000909.2	9	12	**<0.01**	**<0.01**	**<0.01**	**<0.01**	0.30	0.38	0.27	0.33
Proteasome alpha 5 subunit	NP_002781.2	4	3	0.13	0.08	0.01	**<0.01**	0.88	0.86	0.75	0.66
Proteasome beta 3 subunit	NP_002786.2	3	2	0.81	0.02	**<0.01**	**0.01**	1.04	0.60	0.41	0.50
Pyruvate kinase, muscle isoform 2	NP_872271.1	13	12	0.05	0.03	0.02	0.02	0.48	0.40	0.36	0.36
Ribophorin I precursor	NP_002941.1	6	14	0.02	0.63	0.02	0.03	0.22	0.82	0.21	0.22
Ribosomal protein L3 isoform a	NP_000958.1	4	9	0.03	0.03	0.96	0.24	0.13	0.13	0.98	0.57
Ribosomal protein L4	NP_000959.2	12	10	0.29	0.02	0.04	0.05	1.04	0.86	0.91	0.87
Ribosomal protein P0	NP_444505.1	9	7	0.04	0.04	0.21	0.03	0.50	0.51	1.42	0.48
Septin 9 isoform e	NP_001106964.1	3	16	0.72	0.01	0.10	**<0.01**	0.97	0.77	0.81	0.63
Small nuclear ribonucleoprotein polypeptide	NP_073716.1	4	3	0.18	0.02	0.24	**0.01**	1.08	0.86	0.93	0.72
Synaptotagmin binding, cytoplasmic RNA interacting protein	NP_006363.3	7	14	0.07	0.86	0.02	0.01	0.55	0.94	0.34	0.30
Tropomyosin 4	NP_003281.1	3	5	0.65	0.03	0.99	0.03	0.92	0.63	1.00	0.43
Voltage-dependent anion channel 3	NP_005653.3	3	4	**<0.01**	0.49	**<0.01**	0.99	0.45	1.21	0.48	1.00
Group (v)											
ARP3 actin-related protein 3 homolog	NP_005712.1	5	10	0.47	0.28	**0.01**	0.04	1.03	0.93	0.85	0.83
Chaperonin containing TCP1, subunit 4 (delta)	NP_006421.2	5	13	0.16	0.92	**<0.01**	0.03	1.27	0.98	2.07	1.55

Description	NCBI accession number	Number of Peptides	Slice	Probability				Fold change			
				D	L	R	T	D/C	L/C	R/C	T/C
Enolase 1	NP_001419.1	4	11	0.02	**<0.01**	0.63	0.17	1.71	0.62	1.10	0.78
Glutathione transferase	NP_000843.1	4	3	0.23	0.50	**<0.01**	**<0.01**	0.72	1.18	3.06	2.31
Histone cluster 1, H2bi	NP_003516.1	4	1	0.01	0.04	0.25	0.57	0.15	0.37	1.36	0.81
Keratin 9	NP_000217.2	6	18	0.15	0.53	0.03	**<0.01**	0.63	1.48	1.82	19.26
Keratin 9	NP_000217.2	11	10	0.14	0.98	0.02	**0.01**	0.78	1.01	0.66	4.97
Matrin 3 [	NP_061322.2	3	19	0.07	0.88	0.02	0.05	1.78	1.05	0.13	0.27
Mitochondrial ATP synthase, O subunit precursor	NP_001688.1	3	2	0.10	0.95	0.02	**<0.01**	0.90	1.01	1.16	1.21
Myosin IB	NP_036355.2	3	19	0.09	0.07	0.02	0.03	1.47	1.51	0.33	0.40
PREDICTED: similar to Elongation factor 1-gam	xP_001129635.1	16	10	0.20	0.59	0.04	0.03	1.05	0.97	0.88	0.85
Proteasome 26S ATPase subunit 2	NP_002794.1	12	10	0.08	0.24	**<0.01**	0.02	1.07	0.95	0.87	0.77
Ribosomal protein S4, X-linked X isoform	NP_000998.1	7	4	0.45	0.84	**0.01**	**<0.01**	0.94	1.02	0.73	0.72
Ribosomal protein S8	NP_001003.1	3	4	0.90	0.62	**<0.01**	0.02	1.05	0.81	3.12	2.15
Serine (or cysteine) proteinase inhibitor	NP_001226.2	6	10	**<0.01**	**<0.01**	0.26	0.63	1.50	1.31	1.09	0.94

Table 7. Characteristics of proteins classified as those in the group: Nucleoside, nucleotide and nucleic acid metabolism.

Description	Accession	Function
Group (i)		
Adenylosuccinate synthetase isozyme 2	NP_001117.2	Plays an important role in the de novo pathway of purine nucleotide biosynthesis. Catalytic activity: GTP + IMP + L-aspartate = GDP + phosphate + N(6)-(1,2-dicarboxyethyl)-AMP. Location : Cytoplasm.
ATP-dependent RNA helicase A	NP_001348.2	Unwinds double-stranded DNA and RNA in a 3' to 5' direction. Functions as a transcriptional activator. Component of the CRD-mediated complex that promotes MYC mRNA stability. Location : Nucleus › nucleolus. Cytoplasm.
Chromatin-specific transcription elongation factor	NP_009123.1	Involved in multiple processes that require DNA as a template such as mRNA elongation, DNA replication and DNA repair. During transcription elongation as a complex it acts as a histone chaperone destabilizing and restoring nucleosomal structure. Facilitates the passage of RNA polymerase II and transcription by promoting the dissociation of one histone H2A-H2B dimer from the nucleosome, then subsequently promotes the reestablishment of the nucleosome following the passage of RNA polymerase II.
Cold inducible RNA binding protein	NP_001271.1	Involved in cold-induced suppression of cell proliferation. Plays a protective role in the genotoxic stress response, stabilizes transcripts of genes involved in cell survival. Acts as a translational activator and repressor. Translocates from the nucleus to the cytoplasm into stress granules upon various cytoplasmic stresses, such as UV radiation. osmotic and heat shocks.
COP9 signalosome subunit 5	NP_006828.2	Protein stability. An essential regulator of the ubiquitin conjugation pathway. The complex is also involved in phosphorylation of p53/TP53, c-jun/JUN, IkappaBalpha/NFKBIA, ITPK1 and ICSBP, possibly via its association with CK2 and PKD kinases. CSN-dependent phosphorylation of TP53 and JUN promotes and protects degradation by the Ublquitin system, respectively. Location : Cytoplasm. Nucleus.
DNA mismatch repair protein Msh6	NP_000170.1	Component of the post-replicative DNA mismatch repair system (MMR). Heterodimerizes with MSH2 to form MutS alpha, which binds to DNA mismatches this initiates DNA repair. also classified as a protein involved in developmental processes) Location : Nucleus (
DNA repair protein RAD50	NP_597816.1	Component of the MRN complex, plays a central role in double-strand break (DSB) repair,
Family with se quence similarity 98, member B (FAM98B)	NP_775882.2	Protein binding, Pathway biological process mrna splicing
General transcription factor II, i isoform 3	NP_127494.1	Interacts with the basal transcription machinery by coordinating the formation of a multiprotein complex at the C-FOS promoter, and linking specific signal responsive activator complexes. Localised in cytoplasm / nucleus
Heterogeneous nuclear ribonucleoprotein C1/C2	NP_001070910.1	Binds pre-mRNA and nucleates the assembly of 40S hnRNP particles. Single HNRNPC tetramers bind 230-240 nucleotides. Trimers of HNRNPC tetramers bind 700 nucleotides
Heterogeneous nuclear ribonucleoprotein D0	NP_001003810.1	Binds with high affinity to RNA molecules that contain AU-rich elements (AREs) found within the 3'-UTR of many proto-oncogenes and cytokine mRNAs. Also binds to double- and single-stranded DNA sequences in a specific manner and functions a transcription factor. Location :Nucleus, Cytoplasm
Nuclear autoantigenic sperm protein	NP_002473.2	Required for DNA replication, normal cell cycle progression and cell proliferation. Forms a cytoplasmic complex with HSP90 and H1 linker histones and stimulates HSP90 ATPase activity. Also classified in intracellular protein traffic category Location : Cytoplasm
Phosphoribosylformylglycinamidine synthase	NP_036525.1	Pureine metabolism. This enzyme belongs to the family of ligases, specifically those forming carbon-nitrogen bonds carbon-nitrogen ligases with glutamine as amido-N-donor.
Probable ATP-dependent RNA helicase	NP_055644.2	Plays an essential role in splicing, either prior to, or during splicing A complex formation: Location : Nucleus
Prohibitin	NP_002625.1	Inhibits DNA synthesis and has a role in regulating proliferation, mitochondrial respiration activity and in aging (also classified as a cell cycle protein). Location : Mitochondrion inner membrane
Splicing factor 3b, subunit 3	NP_036558	Subunit of the splicing factor SF3B required for 'A' complex assembly formed by the stable binding of U2 snRNP to the branch point sequence (BPS) in pre-mRNA. Location: Nucleus.

Squamous cell carcinoma antigen	NP_055521.1	Regulates Tat transactivation activity through direct interaction. May be a cellular factor for HIV-1 gene expression and viral replication. Location : Cytoplasm.
Staphylococcal nuclease domain containing 1	NP_055205	Functions as a bridging factor between STAT6 and the basal transcription factor. Plays a role in PIM1 regulation of MYB activity. Functions as a transcriptional coactivator for the Epstein-Barr virus nuclear antigen 2 (EBNA2)* Location : Cytoplasm. Nucleus.
Structural maintenance of chromosomes 3	NP_005436.1	Involved in chromosome cohesion during cell cycle and in DNA repair. Central component of cohesin complex. The cohesin complex is required for the cohesion of sister chromatids after DNA replication. The cohesin complex apparently forms a large proteinaceous ring within which sister chromatids can be trapped. At anaphase, the complex is cleaved and dissociates from chromatin, allowing sister chromatids to segregate. The cohesin complex may also play a role in spindle pole assembly during mitosis and in chromosome movement. Location: Nucleus
SWI/SNF-cmplex subunit	NP_003066.2	Involved in transcriptional activation and repression of select genes by chromatin remodeling (alteration of DNA-nucleosome topology). Location : Nucleus
U5 small nuclear ribonucleoprotein	NP_004805.2	Molecular function protein binding, Location : Nucleus.
Group (ii)		
ATP-dependent RNA helicase A	NP_001348.2	Unwinds double-stranded DNA and RNA in a 3' to 5' direction. Functions as a transcriptional activator. Component of the CRD-mediated complex that promotes MYC mRNA stability. Location: Nucleus › Nucleolus. Cytoplasm.
Chromatin-specific transcription elongation factor	NP_009123.1	See group (i)
DEK oncogene	NP_003463.1	May have a function in the nucleus.
H2A histone family, member V isoform 1	NP_036544.1	Variant histone H2A which replaces conventional H2A in a subset of nucleosomes. Nucleosomes wrap and compact DNA into chromatin, limiting DNA accessibility to the cellular machineries which require DNA as a template. Histones thereby play a central role in transcription regulation, DNA repair, DNA replication and chromosomal stability. DNA accessibility is regulated via a complex set of post-translational modifications of histones, also called histone code, and nucleosome remodeling. May be involved in the formation of constitutive heterochromatin. May be required for chromosome segregation during cell division Subcellular location: Nucleus
Splicing factor proline/ glutamine rich	NP_005057.1	DNA- and RNA binding protein, involved in several nuclear processes. Essential pre-mRNA splicing factor required early in spliceosome formation and for splicing. Subcellular location: Nucleus matrix
Group (iii)		
Splicing factor 3B subunit 3	NP_036558	See Nucleoside, nucleotide and nucleic acid metabolism (group 1)
Group (iv)		
Dihydropyrimidinase-related protein 2	NP_001377	Necessary for signaling by class 3 semaphorins and subsequent remodeling of the cytoskeleton. Plays a role in axon guidance, neuronal growth cone collapse and cell migration By similarity. Subcellular location : Cytoplasm.
Heterogeneous nuclear ribonucleoprotein Q	NP_006363	Heterogenous nuclear ribonucleoprotein (hnRNP) implicated in mRNA processing mechanisms. Subcellular location : Cytoplasm. Microsome. Endoplasmic reticulum By similarity. Nucleus
Non-POU domain-containing octamer-binding protein	NP_031389	DNA- and RNA binding protein, involved in several nuclear processes. Subcellular location Nucleus.

Nuclease-sensitive element-binding protein 1	NP_004550	Binds to splice sites in pre-mRNA and regulates splice site selection. Binds and stabilizes cytoplasmic mRNA. Contributes to the regulation of translation by modulating the interaction between the mRNA and eukaryotic initiation factors. Subcellular location : Cytoplasm. Nucleus.
Nucleolin	NP_005372	The major nucleolar protein of growing eukaryotic cells. It is found associated with intranucleolar chromatin and pre-ribosomal particles. It induces chromatin decondensation by binding to histone H1. It is thought to play a role in pre-rRNA transcription and ribosome assembly. May play a role in the process of transcriptional elongation. Subcellular location: Nucleus › nucleolus. Cytoplasm.
Small nuclear ribonucleoprotein-associated protein N	NP_073716	May be involved in tissue-specific alternative RNA processing events. Subcellular location Nucleus.
Trifunctional purine biosynthetic protein adenosine-3	NP_780294	Involved in purine metabolism
Group (v)		
ATP synthase subunit O, mitochondrial	NP_001688	Mitochondrial membrane ATP synthase produces ATP from ADP in the presence of a proton gradient across the membrane which is generated by electron transport complexes of the respiratory chain. Subcellular location : Mitochondrion

General Discussion

Pyrethrins and pyrethroids are acutely neurotoxic by interacting with Na+ channels. Hence, these compounds may comprise a common mechanism group (CMG). There are multiple Na+ channels and other cellular targets, such as voltage activated Ca+ channels, which may also be affected. In addition to perturbing ion transport, exposure of neurones to low levels of pyrethroids can result in changes in the expression of proteins involved in stress response, including apoptosis (Neiderer et al, 2005; Wu et al, 2003) and such effects can be observed in cultured neuronal cells (Wu et al, 2003). Hence, the programme of work described here was conceived where the protein profiles of cells treated with each of the pyrethroids were compared to determine whether the pyrethroids had a common effect or could be classified into different CMGs. The aim was not to examine the effect of the pyrethroids directly on the ion channels and receptors. Such studies are best performed using more specifically directed approaches. We chose to evaluate changes in protein profiles using SH-SY5Y and SK-N-SH cells, which are both derived from a human neuroblastoma. These cell models have been well studied and retain many neuronal properties. We chose to use the technique of surface-enhanced laser desorption/ionization time of flight (SELDI-TOF) mass spectrometry to determine the protein profiles of treated cells. We had previously used this approach successfully to identify protein profiles in human neuronal cells exposed to acrylamide and methylmercury (Fang et al, 2007). We had found that this technique is rapid, reproducible, quantifiable (Abdul-Salam et al, 2006), allows direct sample comparison, can analyse a wide range of proteins including those with masses of 2.5 kDa – 100 kDa, soluble and membrane-bound, acidic and basic proteins. The approach is unbiased and makes no prior assumption of the mechanism(s) of toxicity, nor that a single target is necessarily involved. The main drawbacks with the SELDI-TOF MS approach are the lack of identification of the detected proteins and an analytical sensitivity that favours lower mass proteins. However, this is one of the few proteomic approaches that is capable of relatively high throughput and thus was deemed suitable to undertake the first phase of this investigation. To address the drawbacks we also used a label-free quantitative proteomic approach that employed the use of a tandem MS. The low throughput nature of this technique limited the range of pyrethroids that could be examined, but where applied provided unambiguous identification of responsive proteins. It was important to apply appropriate statistical analyses in order to investigate changes in protein profiles following treatment. The data are complex and required application of various multivariate methods which were directed at addressing the question of whether it was possible to define classification based on the effects of the different compounds on the protein profiles. Based on the responsive proteins identified by tandem MS attempts were made to deduce the pathways involved.

Analysis by both SELDI-TOF MS and label-free proteomics using LC-tandem MS indicated that the protein profile of the SH-SY5Y cell line is responsive to treatment with pyrethroids. Changes in protein levels detected by SELDI-TOF MS analysis were relatively modest. Multivariate analyses were performed in order to investigate whether information from any groups of proteins might be combined to classify the effects of pyrethroids into subgroups that might define CMGs. A number of exploratory investigations were carried out. In general, no obvious classifications were apparent. This appeared to be due to the small magnitude of changes and also the co-correlation in changes in the proteins meaning that little or no increase in classification performance could be derived by combining data from different proteins. However, it was noted that a co-ordinated shift in the levels of a large proportion of the protein levels occurred with half of the pyrethroids which was not evident with the other half. This suggested a novel classification based on this observation and indicated that the pyrethroids studied may comprise more than one CMG. The label-free proteomic approach indicated that there were also some protein changes of greater magnitude. Some of the responsive proteins identified were found to have a function in nucleoside and nucleic acid metabolism, which may be related to the toxicity of these compounds. It is possible that some of these changes may represent an adaptive cellular repair response following exposure to pyrethroids. However, it is important to note that throughout this work non-cytotoxic concentrations of the pyrethroids were used and in many cases there were differences, and sometimes contrary effects, in the adaptive response of proteins to different pyrethroids. Specifically, it was shown that the levels of many proteins varied differently in response to deltamethrin and cyhalothrin compared with the response

to resmethrin and tetramethrin. This suggests that many of the effects were not an unspecific response to a toxic insult but rather an (adaptive) response appropriate to the compound administered.

The suitability of the cell lines selected for use should be considered. The lack of a functional response of the SK-N-SH cells to pyrethroids as determined by noradrenline release and glucose uptake together with a lack of effect on protein profiles suggests that this cell line was not suitable for these studies. However, noradrenline release, but not glucose uptake, was affected in SH-SY5Y cells as were protein profiles. In both cases the cells were used for studies after a period of relatively short term culture and under such conditions the cells appeared healthy, with a rounded appearance. We have shown previously that under conditions of prolonged culture in a nutrient poor medium the cells will take on a more differentiated phenotype with the appearance of dendritic projections. It is possible that in this condition the cells may react differently and possibly more appropriately to treatment with pyrethroids. Unfortunately though, the time taken for the differentiation to occur, and the amount of cell loss that occurs over this time, limits the type of experiment that can be performed. Previous attempts to perform proteomic studies on such cells were unsuccessful as it was not possible to recover a sufficient number of differentiated cells to perform the analysis. This might be addressed by increasing the scale of the cultures by one or two orders of magnitude, although this would be costly. Similarly, it might also be possible to construct more complex neuronal models comprising different cell types. Possibly, such models might yield more pertinent information, but this project did not set out to develop such models. Consequently, for simplicity and pragmatism undifferentiated human SH-SY5Y and SK-N-SH cells were used in these studies. The use of rodent cell lines was not considered appropriate as the aim of this work was to generate data more directly applicable to humans. However, if some of the changes found can be validated it would be of interest to see if these could be reproduced in rats or possibly rat cell lines and this may help explain T-and CS syndromes.

Further work should be performed in order to validate the proteomic findings. Initially, the levels of those proteins that appear to change on exposure to pyrethroids should be confirmed using independent methods of quantification. To confirm their mechanistic role specific studies should be conducted that manipulate levels in some way and to assess the impact on the response of the cell to various pyrethroids. At the outset of this project we suggested the use of siRNA. Unfortunately, the identification of the responsive proteins was obtained only some months after the completion of the contract and so there was no time to design and implement any such experiments.

Conclusions

Analysis by both SELDI-TOF MS and label-free proteomics using LC-tandem MS indicated that the protein profile of the human neuroblastoma cell line, SH-SY5Y, is responsive to treatment with pyrethroids. Further, this work suggests some differences in the effects of the different pyrethroids studied and that they may comprise more than one CMG. Interestingly, the responsive proteins include many that have a function in nucleoside and nucleic acid metabolism and this may relate to the toxicity of these compounds. Further work would be necessary to define the membership of such CMGs and to determine the mechanism(s) that cause the changes in protein expression and their biological consequences.

References

Abdul-Salam VB, Paul GA, Ali JO, Gibbs SR, Rahman D, Taylor GW, Wilkins MR, and Edwards RJ (2006). Identification of plasma protein biomarkers associated with idiopathic pulmonary arterial hypertension. *Proteomics* 6:2286-2294.

Amweg EL, Weston DP, Ureda NM (2005). Use and toxicity of pyrethroid pesticides in the central valley, California USA. *Environ.Toxicol.Chem* 24: 966–972.

ATSDR (2003). Toxicological profile of pyrethrins and pyrethroids. Agency for Toxic Substances and Disease Registry (ATSDR), US Department of Health and Human Services, Atlanta GA.

Barzilai A, Biton S, and Shiloh Y (2008). The role of the DNA damage response in neuronal development, organization and maintenance. *DNA Repair* 7: 1010–1027.

Bradberry SM, Cage SA, Proudfoot AT, Vale JA (2005). Poisoning due to pyrethroids. *Toxicol Rev* 24:93-106.

Breckenridge CB, Holden L, Sturgess N, Weiner M , Sheets L, Sargent D, Soderlund DM, Choi JS, Symington S, Marshall Clark, J, Burr S, Ray D (2009). Evidence for a separate mechanism of toxicity for the Type I and the Type II pyrethroid insecticides. *J NeuroToxicology* 30S:S17–S31.

Casida JE (1970). Mixed-function oxidase involvement in the biochemistry of insecticide synergists. *J. Agr. Food Chem* 18:753-772.

Coats JR (1990). Mechanisms of toxic action and structure-activity relationships for organochlorine and synthetic pyrethroid insecticides. *Environ Health Perspect* 87:255-262.

Crofton KM, Reiter LW (1988). The effects of type I and II pyrethroids on motor activity and the acoustic startle response in the rat. *Fundam Appl Toxicol* 10:624-634.

Crofton KM, Reiter LW, Mailman RB (1987) Pyrethroid insecticides and radioligand displacement from the GABA receptor chloride ionophore complex. *Toxicol Lett* 35:183-90.

Cui X, Churchill GA (2003). Statistical tests for differential expression in cDNA microarray experiments *Biology* 4:210.

Elliott M, Janes NF, Potter C (1978). The future of pyrethroids in insect control. *Ann. Rev. Entomol*. 23:443-69.

Fang M, Boobis AR, and Edwards RJ (2007). Searching for novel biomarkers of centrally and peripherally-acting neurotoxicants, using surface-enhanced laser desorption/ionisation-time-of-flight mass spectrometry (SELDI-TOF MS). *Food Chem Toxicol* 45:2126-2137.

Francisconi S, Codenotti M, Ferrari-Toninelli G, Uberti D, Memo M (2005). Preservation of DNA integrity and neuronal degeneration. *Brain Research Reviews* 48:347-351.

Fortin MC, le Bouchard M, Carrier G, Dumas P (2008). Biological monitoring of exposure to pyrethrins and pyrethroids in a metropolitan population of the Province of Quebec, Canada. *Environmental Research* 107: 343–350.

Gammon DW, Brown MA, Casida JE (1981). Two classes of pyrethroid action in the cockroach.

Pestic. Biochem. Physiol 15:181–191.

Gray AJ (1985). Pyrethroid structure-toxicity relationships in mammals. *Neurotoxicology* 6:127-137.

Hildebrand ME, McRory JE, Snutch TP, Stea A (2004). Mammalian voltage-gated calcium channels are potently blocked by the pyrethroid insecticide allethrin. *JPET* 308: 805-813.

Issaq HJ, Conrads TP, Prieto DA, Tirumalai R, Veenstra TD (2003). SELDI-TOF MS for diagnostic proteomics. *Analytical Chemistry* 75:148A-155A.

Joy RM, Albertson TE, Ray DE (1989). Type 1 and Type II pyrethroids increase inhibition in the hippocampal dentate gyrus of the rat. *Toxicology and Applied Pharmacology* 98:398-412.

LaForge FB, Markwood LN (1938). Organic insecticides. *Annu. Rev. Biochem* 7:473–490.

Lawrence, LJ and Casida, JE (1982). Pyrethroid toxicology: Mouse intracerebral structure-toxicity relationships. *Pestic. Biochem. Physiol* 18: 9-14.

Lawrence LJ, Casida JE (1983) Stereospecific action of pyrethroid insecticides on the gamma-aminobutyric acid receptor-ionophore complex. *Science* 221:1399-401.

Lleonart ME (2010). A new generation of proto-oncogenes: Cold-inducible RNA binding proteins *Biochim Biophys Acta* 1805: 43–52.

Macan J, Varnai VM, Turk R (2006). Health effects of pyrethrins and pyrethroids. *Arh Hig Rada Toksikol* 57:237-43.

Mannerstrom M, Tahti H (2004). Modulation of glucose uptake in glial and neuronal cell lines by selected neurological drugs. *Toxicol Lett* 151:87-97.

Metcalf RL (1995). Insect control technology. In: Kirk-Othmer encyclopedia of chemical technology. New York: John Wiley and Sons, pp 533-602.

Metz CE (1978). Basic principles of ROC analysis. *Seminars in Nuclear Medicine* 8:283-298.

Miyamoto J (1976). Degradation, metabolism and toxicity of synthetic pyrethroids. *Environ Health Perspect* 14:15-28.

Miyamoto J, Kaneko H, Tsuji R, Okuno Y (1995). Pyrethroids, nerve poisons: How their risks to human health should be assessed. *Toxicol Lett* 82:933-940.

Mosmann T (1983). Rapid colorimetric assay for cellular growth and survival: application to proliferation and cytotoxicity assays. *J Immunol Methods* 65:55-63.

Narahashi T (2000). Neuroreceptors and ion channels as the basis for drug action: Past, present and future. *J Pharmacol Exp Ther* 294: 1–26.

Niederer KE, Morrow DK, Gettings JL, Irick M, Krawiecki A, Brewster JL (2005). Cypermethrin blocks a mitochondria-dependent apoptotic signal initiated by deficient N-linked glycosylation within the endoplasmic reticulum. *Cell Signal* 17:177-186.

Seyedi N, Mackins CJ, Machida T, Reid AC, Silver RB, Levi R (2005). Histamine H3-receptor-induced attenuation of norepinephrine exocytosis: a decreased protein kinase a activity mediates a reduction in intracellular calcium. *J Pharmacol Exp Ther* 312:272-280.

Shafer TJ, Meyer DA (2004). Effects of pyrethroids on voltage-sensitive calcium channels: a critical evaluation of strengths, weaknesses, data needs, and relationship to assessment of cumulative neurotoxicity.*Toxicol Appl Pharmacol* 196:303-18.

Soderlund DM (1992). Metabolic considerations in pyrethroid design. *Xenobiotica* 22: 1185-1194.

Soderlund DM, Clark JM, Sheets LP, Mullin LS, Piccirillo VJ, Sargent D, Stevens JT, Weiner ML (2002). Mechanisms of pyrethroid neurotoxicity: Implications for cumulative risk assessment. *Toxicology* 171:3–59.

Tang N, Tornatore P, Weinberger SR (2004). Current developments in SELDI affinity technology. *Mass spectrometry reviews* 23 (1): 34–44.

Verschoyle RD, Aldridge WN (1980). Structure-activity relationships of some pyrethroids in rats. *Arch Toxicol* 45:325-329.

Vijverberg HP, van den Bercken (1990). Neurotoxicological effects and the mode of action of pyrethroid insecticides. *Crit Rev Toxicol* 21:105–126.

Wolansky MJ, Gennings C, DeVito MJ, Crofton KM (2009). Evidence for dose-additive effects of pyrethroids on motor activity in rats. *Environ Health Perspect* 117:1563-1570.

Wright CD, Forshaw PJ, Ray DE (1988). Classification of the actions of the ten pyrethroid insecticides in the rat, using the trigeminal reflex and skeletal muscle as test systems. *Pestic Biochem Physiol* 30:79-86.

Wu A, Li L, Liu Y (2003). Deltamethrin induces apoptotic cell death in cultured cerebral cortical neurons. *Toxicol Appl Pharmacol* 187:50-57.

Zhu Z, Edwards RJ, Boobis AR (2009). Increased expression of histone proteins during estrogen-mediated cell proliferation. *Environ Health Perspect* 117:928-34.